MARTIN MARIETTA ENERGY SYSTEMS LIBRARIES
3 4456 0364463 4

[redacted]

ORNL-3211
C-44a – Nuclear Technology – Materials
M-3679 (25th ed.) 145

OAK RIDGE NATIONAL LABORATORY

STATUS AND PROGRESS REPORT

SEPTEMBER 1961

CENTRAL RESEARCH LIBRARY
DOCUMENT COLLECTION
LIBRARY LOAN COPY
DO NOT TRANSFER TO ANOTHER PERSON
If you wish someone else to see this document, send in name with document and the library will arrange a loan.

OAK RIDGE NATIONAL LABORATORY
operated by
UNION CARBIDE CORPORATION
for the
U.S. ATOMIC ENERGY COMMISSION

[redacted]
Downgrade to Unclassified After October 5, 1962

LEGAL NOTICE

This report was prepared as an account of Government sponsored work. Neither the United States, nor the Commission, nor any person acting on behalf of the Commission:

A. Makes any warranty or representation, expressed or implied, with respect to the accuracy, completeness, or usefulness of the information contained in this report, or that the use of any information, apparatus, method, or process disclosed in this report may not infringe privately owned rights; or

B. Assumes any liabilities with respect to the use of, or for damages resulting from the use of any information, apparatus, method, or process disclosed in this report.

As used in the above, "person acting on behalf of the Commission" includes any employee or contractor of the Commission, or employee of such contractor, to the extent that such employee or contractor of the Commission, or employee of such contractor prepares, disseminates, or provides access to, any information pursuant to his employment or contract with the Commission, or his employment with such contractor.

[redacted]

ORNL-3211

Copy No._____

Contract No. W-7405-eng-26

OAK RIDGE NATIONAL LABORATORY

STATUS AND PROGRESS REPORT

SEPTEMBER 1961

DATE ISSUED OCT 9 1961

OAK RIDGE NATIONAL LABORATORY
Oak Ridge, Tennessee
operated by
UNION CARBIDE CORPORATION
for the
U.S. ATOMIC ENERGY COMMISSION

[redacted]

MARTIN MARIETTA ENERGY SYSTEMS LIBRARIES

3 4456 0364463 4

CONTENTS

REACTOR DEVELOPMENT PROGRAM..... 1
GAS-COOLED REACTOR PROJECT..... 1
EGCR Development Studies..... 1
Fuel Material Irradiation Studies..... 1
Radiation Effects on Stainless Steel..... 2
Radiation Effects on BeO..... 2
GCR-ORR Loop No. 1..... 3
GCR-ORR Loop No. 2..... 3
Test of Thermocouples at High Temperatures..... 3
Inspection of Finned Beryllium Tubing..... 3
THORIUM UTILIZATION PROGRAM..... 3
Planning and Evaluation Studies..... 3
Engineering of Thorium Reactor Systems..... 4
Homogeneous Reactor Experiment No. 2..... 4
MOLTEN-SALT REACTOR PROGRAM..... 4
MSRE Design: Components, Systems, and Structures..... 4
MSRE Design: Maintenance Equipment..... 4
MSRE Design: Instrumentation..... 4
MSRE Procurement and Construction..... 5
Chemical Development..... 5
Irradiation Tests..... 6
Heat Transfer and Physical Properties of Molten Salts..... 6
PEBBLE-BED REACTOR..... 6
Reactor Physics..... 6
Core Design..... 7
Pressure Vessel Stress Analyses..... 7
STUDIES AND EVALUATIONS..... 7
Reactor Evaluation Studies..... 7
ADVANCED REACTOR DEVELOPMENT..... 8
Advanced Test Reactor Corrosion Program..... 8
High Flux Isotope Reactor Design and Development..... 8
Physics..... 8
Control and Instrumentation..... 10
Metallurgy..... 10
Design..... 10
Critical Experiments..... 11
NUCLEAR TECHNOLOGY AND GENERAL SUPPORT..... 12
Nondestructive Test Development..... 12
Mechanical Properties Research..... 12
Solid Reaction Studies..... 12
Fuel Element Development..... 13
Reactor Controls Development..... 13
Power Reactor Fuel Processing: Solvent Extraction..... 14
Power Reactor Fuel Processing: Zirconium-Containing Fuel..... 15
Power Reactor Fuel Processing: Uranium-Graphite and Uranium Carbide Fuels..... 15

Power Reactor Fuel Processing: Mechanical..... 16
Power Reactor Fuel Processing: Beryllium- and BeO-Containing Fuels..... 16

PHYSICAL RESEARCH PROGRAM..... 17
Reactor Operations..... 17
Waste Disposal..... 17
Hot-Cell Operations..... 17
PHYSICS AND MATHEMATICS RESEARCH..... 17
Charge Spectrometry..... 17
Neutron Diffraction..... 18
Fast-Chopper Time-of-Flight Spectrometer..... 18
High-Voltage Experimental Program: Coulomb Excitation of Osmium and Chromium Nuclei..... 18
High-Voltage Experimental Program: The $C^{13}(He^3,n)O^{15}$ Reaction..... 19
CHEMISTRY RESEARCH..... 19
Effects of Radiation on Analytical Methods..... 19
Spectrophotometric Studies of Solutions at Elevated Temperatures and Pressures..... 19
Volatility Studies..... 20
Solvent Extraction Research..... 20
Nuclear Methods of Chemical Analysis..... 21
Organic Chemistry..... 22
Chemistry of the Heavy Elements..... 22
Radiation Chemistry..... 22
Electrochemical Kinetics and Its Application to Corrosion..... 23
High-Temperature Aqueous Solution Chemistry..... 23
Physical Chemistry of Molten Salts: Cryoscopy in Fluoride Systems..... 24
Physical Chemistry of Molten Salts: Association in Nitrate Systems..... 24
Chemical Separation of Isotopes..... 25
Chemical Applications of Nuclear Explosions..... 25
METALLURGY AND MATERIALS RESEARCH..... 26
Metallurgy of Superconducting Materials..... 26
Ceramics Research: Sintering Studies..... 26
Physical Property Studies..... 27
CONTROLLED THERMONUCLEAR RESEARCH..... 27
DCX-1 Facility..... 27
High-Current Injection..... 28
Theory..... 28
Radio-Frequency Heating..... 28

BIOLOGY AND MEDICINE PROGRAM..... 29
SOMATIC EFFECTS OF RADIATION..... 29
Pathology and Physiology: Recovery from Somatic Effects of Radiation..... 29
RADIATION GENETICS..... 29
Mutagen Mechanisms: Bacterial Genetics..... 29
COMBATING DETRIMENTAL EFFECTS OF RADIATION..... 29
Mammalian Recovery: General..... 29

Mammalian Recovery: Mammalian Cytology and Genetics in Vitro..... 30
Radiation Immunology..... 30
MOLECULAR- AND CELLULAR-LEVEL STUDIES..... 31
Cell Growth and Reproduction..... 31
Biophysics: Ultraviolet Studies..... 31
Biophysics: Vacuum Ultraviolet Studies..... 31
Biophysics: Electron Spin Resonance Studies..... 31
RADIOLOGICAL PHYSICS, HEALTH PHYSICS, AND INSTRUMENTATION.... 31
Basic Instrumentation..... 31

OPEN LITERATURE PUBLICATIONS..... 33

VISITORS..... 36

[redacted]

OAK RIDGE NATIONAL LABORATORY

STATUS AND PROGRESS REPORT

SEPTEMBER 1961

This Status and Progress Report summarizes that portion of the Laboratory's work which is unclassified. Some of the topics are included every month, but the majority are reported on a bimonthly schedule.

REACTOR DEVELOPMENT PROGRAM

GAS-COOLED REACTOR PROJECT

EGCR Development Studies. — The steady-state thermal stresses in an EGCR graphite column were calculated and found to be negligible, as anticipated.

Satisfactory operation of the 6-in.-IPS hermetically sealed gate valve was achieved. The valve is now being thermally cycled between 200 and 1050°F with 1000 psig internal pressure.

The cause and the extent of cracking in the casings of the pressure-vessel cooling compressors, as reported by the fabricators, were investigated. One casing had seven cracks on the external surface adjacent to the nozzle weld, and the other had four cracks in the same general location. The most severe crack in each casing was slightly less than 1/4 in. deep and about 2 in. long. All the cracks were successfully removed by grinding. It was determined that the cracking resulted from tack welding the nozzle into place without proper preheating of the parts. The backing rings are being ground out to permit inspection of the internal surface areas before the welding is continued.

Fuel Material Irradiation Studies. — Metallographic examinations of both UC_2-graphite matrix fuel pellets irradiated in capsule MTR-48-1 confirmed the fuel concentration gradient indicated by core drill samples. The fuel concentration was at a maximum near the center of the pellet and decreased toward the edge. Less fuel burnup was expected at the center because of flux depression across the pellet. At low magnification the microstructures of the "a" and "b" pellets were similar to that of the unirradiated control. High magnification, however, showed that the irradiated UC_2 particles had lost their angular appearance; spheroidization appeared to have taken place. Metallographic examination of the graphite can failed to show the presence of uranium, which had been found by analysis of core drillings.

Metallographic observations of fuel distribution in the UC_2-graphite matrix of fuel pellets irradiated in capsule MTR-48-2 agreed fairly well with core-drilling results. The appearance of fuel pellet "b" was different from that of MTR-48-1 pellets in that a portion of the UC_2 migrated

[redacted]

into the graphite matrix and the remainder spheroidized. No uranium was found in the graphite can by metallographic techniques, but a thin layer (about 0.5 mil thick) of an unidentified material was seen on the inner surface of the graphite can.

Examination of the material found on the outer surface of MTR-48-2 fuel pellets failed to yield a positive identification. The silver-colored globules, similar to mercury in appearance, appeared to have a melting point near room temperature. They reacted strongly with water, releasing gas and leaving a black powder residue. Results of radiochemical analysis of a sample, in atoms per sample, were: uranium, 2.03×10^{18}; Ce^{144}, 5.36×10^{16}; Zr^{95}, 5.35×10^{14}; Cs^{137}, 2.41×10^{14}; Sr^{89}, 1.74×10^{14}. When another sample was examined by emission spectroscopy, the major constituent was found to be lanthanum. The other constituents, in order of decreasing amounts, were Ce, Na, Be, Y, Zr, and Si.

The ORNL-MTR-48-5 irradiation test is in the third three-week MTR irradiation cycle. The fuel consists of a dispersion of pyrolytic-carbon-coated 175- to 250-μ UC_2 particles in a graphite matrix. During the past month the experimental assembly was operated at a graphite bottle wall temperature of 1500 ± 50°F, a fission power of ~2.75 kw, and a central temperature of 2500°F.

Irradiation of experimental assembly L-M5ab was completed and the unit was removed from the LITR core on August 22. This capsule contains BeO-UO_2-ThO_2 ceramic fuel. Examination of miniature capsule L-M3, containing UO_2-ThO_2-BeO dispersion fuel pellets with ThO_2 insulators, was begun. No defects were seen in the outside of the cladding or the external thermocouples. Fission gas was collected from both sections of the capsule. All four fuel pellets from the "a" section and one pellet from the "b" section were removed intact and measured. Small increases in length and diameter were found; only the pellet from the "b" section showed more than 1% change. The tantalum-sheathed thermocouple in the "b" section was swollen and brittle, and three of the fuel pellets were held tightly in the insulators. This finding indicates capsule leakage during irradiation and may explain the larger dimensional increases of the one pellet from the "b" section. This indication is supported by the fact that much less fission gas was found in the "b" section than in the "a" section.

Beryllium-clad fuel element test assemblies are being prepared for irradiation in the Westinghouse Test Reactor. The test assembly will be a one-half-length EGCR assembly, and it will be operated under the conditions to be experienced by an EGCR beryllium-clad fuel assembly at the highest flux point in a channel.

Radiation Effects on Stainless Steel. — An experimental assembly containing ten tube-burst specimens of type 304 stainless steel tubing was inserted in the poolside facility of the ORR. The specimens are being operated at 1200 to 1500°F.

Radiation Effects on BeO. — Fabrication of BeO irradiation test assembly ORNL-41-7 was completed and final assembly began. Statistical organization of 300 BeO specimens for irradiation in assembly ORNL-41-8 was tentatively formalized. Exposure conditions will be varied to permit evaluation of the temperature annealing effects vs the neutron effects.

GCR-ORR Loop No. 1. – During the shutdown ending on September 3, the primary piping system of GCR-ORR loop No. 1 was brought in line with the final design criteria. The vacuum manifold was completed, a carbon trap was installed in the primary system, and the instrumentation, including that of the nitrogen sweep gas system, was completed. The compressor cubicle and its related surge ducts and tank were made leak-tight and tested, and the loop was completely checked out prior to being operated with the first fueled assembly.

On September 3, the loop was started up with a 25,000-Btu hr^{-1} ft^{-1} instrumented fuel element of a prototype EGCR design in the in-lattice position. The startup was very satisfactory; the maximum temperature of the outer cladding of the element is 1450°F.

GCR-ORR Loop No. 2. – Design and construction work on GCR-ORR loop No. 2 continued as scheduled. Facilities at the ORR for the loop are 87% complete. One of the regenerative compressors was assembled and was found to be leak-tight.

Test of Thermocouples at High Temperatures. – Continued large negative drifts were noted for the type 304 stainless-steel-sheathed Chromel-P–Alumel thermocouples being tested at 870°C in a 7-psig hydrogen atmosphere. After 98 days the average error is –2.7 mv (–67.5°C). Similar thermocouples exposed to a CO atmosphere for 137 days have drifted slightly positive; the error is +6.5°C, but little change in the drift has occurred in the past 30 days.

Inspection of Finned Beryllium Tubing. – Approximately 100 ft of 0.500-in.-ID finned beryllium tubing in 2-ft sections was received for nondestructive evaluation. This tubing has 12 identical external helical fins approximately 1/4 in. high. The minimum wall thickness in the groove between the fins is approximately 0.040 in. Thirty-five of the 50 tubes were accepted, based on fluorescent-penetrant and eddy-current inspections. There seemed to be a pattern of rejection vs extrusion number; 8 of the 15 rejects were from only 2 of the 13 extrusions.

THORIUM UTILIZATION PROGRAM

Planning and Evaluation Studies. – Additional studies were completed for single-region molten-salt converter reactors (MSCR), with C/Th ratios of 125 to 500 and core diameters of 15 to 20 ft. Breeding ratios of 0.5 to 0.7 appear obtainable at economic processing rates. No conditions appear to exist which would limit the power output of a single reactor system to less than 1000 Mw (electrical). Factors considered were the temperature rise in the graphite after shutdown and fuel drainage, temperature rise in the fuel salt following fuel-pump failure, thermal stress in the graphite moderator, circuit pressure drop, and ratio of pump work to reactor power. Preliminary calculations indicate that power removal capabilities of 4 Mw (thermal) per cubic foot of salt can be obtained in the external fuel system; over-all power densities in the fuel salt were about 1.5 Mw (thermal) per cubic foot of fuel salt.

A new equilibrium reactor code (ERC-7) capable of treating converters fueled with U^{235} or Pu^{239} was written and partially checked out. The

new code has improved convergence characteristics, greater flexibility with regard to fuel-processing options, considers specific fission product chains (using effective cross sections based on thermal and resonance cross sections and on relative fast flux), and calculates the fuel-cycle cost.

Engineering of Thorium Reactor Systems. – The friction-factor section of the 200B loop was modified to allow friction factors of thoria slurry to be obtained in the transition- and laminar-flow regions. An additional pressure tap was installed to permit measurement of the pressure drops through either the upstream or downstream half of the friction-factor section.

Rheology of the 0.8-μ slurry previously run in the friction-factor section was measured in a capillary-tube viscometer.

Homogeneous Reactor Experiment No. 2. – Approximately 3000 kg of D_2O was recovered from the HRE-2 fuel solution. The heavy water was satisfactorily decontaminated by two evaporations, followed by an ion exchange treatment. The only significant activity remaining is tritium (approximately 0.2 curie/liter).

The analysis of reactor runs and the preparation of reports continue as the major activities. Preparations are being made for the cutting and removal of sections of the Zircaloy-2 core vessel.

MOLTEN-SALT REACTOR PROGRAM

MSRE Design: Components, Systems, and Structures. – The basic designs and layouts for all components, systems, and facilities of the MSRE are very nearly finished, and the detail drawings are being completed as rapidly as possible.

Major system design effort in September was expended in detailing the thermal-shield water connections and miscellaneous appurtenances, detailing the fuel-pump support, making additions to the coolant circuit, continuing the detailing of off-gas and electrical circuits, and carrying forward instrumentation layout.

Small modifications of tolerances were made on the component drawings. Detailing of control rods and drives continued.

MSRE Design: Maintenance Equipment. – The design concept for the drain-tank jig was completed. Detailing of all jigs and of the television vehicle continues.

MSRE Design: Instrumentation. – A study of data-handling requirements for the MSRE was completed.

Instrument-application drawings for the cooling-water and liquid-waste systems were completed. Eight instrument application drawings and tabulations covering the instrumentation for the main systems were revised and were issued for comment.

Detail layout of the main control panel, detail designs of panels located in auxiliary instrument areas, and preparation of preliminary schematic drawings of the electrical system were begun. Comments received on the conceptual layout drawing of the main control panel indicate that the proposed graphic method of display and presentation is acceptable.

Layouts of the weight-system panels are being made, and a 480-point thermocouple patch panel has been detailed.

A preliminary survey was made of requirements for process and personnel radiation monitors.

Development work continued on liquid-level transmitters: a float type for continuous measurement of molten-salt level in the pump bowls and a conductivity type for single-point measurement of level in the storage tanks. Investigation of methods of attaching Inconel-clad mineral-insulated thermocouples to INOR-8 pipes and vessels is also continuing.

MSRE Procurement and Construction. – The one bid (received from National Carbon Company) for furnishing the MSRE moderator graphite, completely machined, was reviewed and accepted.

A prebid conference was held with seven potential fabricators of major reactor components. The conference resulted in changes to drawings and specifications to reduce fabrication costs. The scheduled bid-opening date is October 10.

Inspection of the INOR-8 plate, rod, and sheet being produced by Haynes Stellite Company has revealed that over half the material inspected does not meet the dimensional or metallurgical requirements of the specifications. Most of the dimensional deviations can be corrected or the material can be accepted without jeopardy to the reactor system. The first shipment of material is scheduled for delivery in mid-October.

Bids to furnish INOR-8 pipe, tubing, and fittings were reviewed and accepted.

Additional changes in drawings and specifications for the lump-sum modifications to Building 7503 extended the bid-opening date to September 19. The bids are being reviewed.

The blowers, motors, and louvers for air cooling the radiator in the reactor coolant system in Building 7503 are being checked and put in operating condition.

Chemical Development. – Strong reducing agents such as zirconium metal could, in principle, be used to shorten the time-consuming treatments (two or three days) with H_2 currently employed to remove oxidizing impurities during fuel manufacture, although the addition of UF_4 would have to be made at a later stage to avoid formation of UF_3. Two of the troublesome points involved in such a procedure were studied. Zirconium in the form of lathe turnings appears to have reacted completely, without interference from deposition of an adhering coat of reduced metal, when added to $LiF\text{-}BeF_2$ melts containing 0.2 wt % of chromium ion. The chromium ions, which are very difficultly reducible by H_2, are partly in the trivalent state, even when in equilibrium with chromium metal, and the fraction of trivalent ions decreases with increasing dilution, as was reflected in the stoichiometry of the reaction with zirconium metal when followed by means of radioactive chromium ion tracers. In the course of treatment with zirconium metal, an as-yet-unidentified black sludge and scum, apparently not predominantly reduced metal, appears in a quantity sufficient to cause considerable difficulty with plugging of filters in transfer lines.

Irradiation Tests. – The third MSRE graphite-fuel capsule experiment (ORNL-MTR-47-3), designed to study the compatibility and wetting characteristics of molten fuel salt with AGOT and R0025 graphites, molybdenum, and INOR-8 in four capsules, was sent to Battelle Memorial Institute for postirradiation examination. The assembly was opened, and the capsule containers were observed to be in good condition.

Preliminary results from examination of two fuel-graphite compatibility-test assemblies, in which the fuel had undergone 8.5% burnup at 200 w/cc and 900°C during the 12-week irradiation period, indicated that a slight distillation of the fuel solvent occurred and that a small amount of CF_4 accumulated in the helium cover gas in the sealed capsules. Otherwise, the graphite boat and INOR-8 container appeared to be in excellent condition.

Heat Transfer and Physical Properties of Molten Salts. – The investigation of the enthalpy of $LiF-BeF_2-ThF_4-UF_4$ (67.0-18.5-14.0-0.5 mole % nominal) salt mixture was continued. Two additional measurements were completed: (1) a rerun with one of the capsules used in the original enthalpy determinations with this salt ("Uncirculated B" in the tabulation below) and (2) a sample taken from a ground and thoroughly mixed portion of the salt used in the heat transfer experiment ("Circulated D" in the tabulation). The results for heat capacity, along with those obtained from previous measurement with an uncirculated sample (A) and with an unmixed sample of circulated salt (C), are as follows:

Sample	Composition $LiF-BeF_2-ThF_4-UF_4$ (mole %)	Heat Capacity [cal g^{-1} $(°C)^{-1}$]
	67.0-18.5-14.0-0.5 (nominal)	
Uncirculated A	70.3-15.4-13.8-0.6	$0.493 - (23.42 \times 10^{-5})t$
Uncirculated B	Not available	$0.548 - (31.58 \times 10^{-5})t$
Circulated C	70.8-16.6-12.1-0.5	$0.354 - (2.74 \times 10^{-5})t$
Circulated D	72.6-15.3-11.7-0.4	$0.607 - (40.88 \times 10^{-5})t$

In contrast to the enthalpy (a maximum variation of ±3.5% around the mean between 550 and 800°C), the heat capacity appears to be quite sensitive to composition changes. The measurements are being re-examined to determine whether this sensitivity is real.

PEBBLE-BED REACTOR

Reactor Physics. – Further calculations have indicated that four 4-in.-diam control rods placed 5 in. outside the outer edge of the core will be required for the PBRE. The circumferential power distribution in the portions of the core affected by control-rod insertion is not severely distorted. The over-all power distribution in the portions of the core affected by the control rods is characterized by a lower peak-to-average power distribution than without the rods because of the effect

of the rods in suppressing the flux peak near the reflector. The total worth of the four rods has been computed to be about 0.218k. In comparison, the required reactivity control from temperature coefficient, fission products, and burnup is estimated to be about 0.068k.

Core Design. – Preliminary calculations have been completed on the coolant-circuit pressure drop, on natural-convection cooling for removal of after-heat, and for bypass flow through a proposed core-reflector configuration. The pressure drop through the reactor system was based on the maximum flow rate of 24,700 lb/hr through the core, plus an additional 20% for control-rod and reflector cooling and for attemperation of the high outlet gas temperature. The total calculated pressure drop was 4 psi.

Natural-convection cooling for after-heat removal appears to be readily achievable at the operating pressure of 500 psia, assuming, of course, that the steam generators are functioning. The steam generator height above the reactor core required to circulate sufficient helium (700°F gas temperature rise) to remove the shutdown decay heat was computed to be about 12 ft. Preliminary design layouts indicate that 20 to 25 ft will be available.

Calculations have also been made for determining the integrated average bed void fraction for the core. Based on experimental data obtained by Sanderson and Porter, the estimated core void fraction is 41.8%.

Pressure Vessel Stress Analyses. – Preliminary analyses of the nozzle penetrations in the pressure vessel were completed, and the required thicknesses for the vessel and nozzles were established, based on the pressure loading alone. The ends of the gas inlet line will be displaced relative to each other as the result of any misalignment between the steam generator and the pressure vessel. Hence, a preliminary examination was made of the stresses in the region of the junction between the gas inlet line and the pressure vessel that are produced by vertical displacement at the steam generator end of the line. Based on an approximation which is believed to be conservative, the maximum discontinuity stress in the nozzle was 287,000δ and the maximum discontinuity stress in the vessel was 114,000δ, where δ is the vertical misalignment between the steam generator and the pressure vessel. If δ were 0.1 in., for example, the stress produced in the nozzle would be 28,700 psi. Initial investigations of the pressure vessel support-lug attachment regions indicate that these may be critical regions for the vessel.

STUDIES AND EVALUATIONS

Reactor Evaluation Studies. – A preliminary report summarizing the work done to date on fuel-value studies was written and forwarded to the AEC for their use in establishing the buy-back price of bred fissile material. Based on calculations analyzed to date, the fuel value of high-purity Pu^{239} was about \$11/g; recycle plutonium had a value of about \$8/g; high-purity U^{233} and U^{233} obtained from the U^{233}-Th cycle had a value of \$15/g; while U^{233} obtained from the U^{235}-Th cycle had a value of about \$13/g. These values may change slightly after new results have been analyzed.

The Sisyphus program, which calculates fuel burnup, isotopic concentrations, and associated fuel costs as a function of time in single-region fluid-fuel reactors, has been completed and is ready for use. It is similar to the Expire-Epitaph programs, except that it maintains criticality by adjusting fuel concentration and determines effective thermal cross sections by means of the Wilkins equation.

ADVANCED REACTOR DEVELOPMENT

Advanced Test Reactor Corrosion Program

Two heat flux-corrosion specimens, 6061 and X8001 aluminum, were tested for 30 days at a heat flux of 1.5×10^6 Btu hr^{-1} ft^{-2} with the cooling water adjusted to a pH of 5.0 with HNO_3. In both cases the coolant flow rate was 45 fps and the surface temperature at the axial midpoint of the specimen was 350°F. During the test the X8001 specimen developed about 3 mils of oxide, which corresponded to a temperature drop over the oxide of about 260°F at the end of the test. Uniform penetration of the aluminum to a depth of about 3 mils was observed. During the test with the 6061, the rate of temperature increase was approximately the same as with the X8001, but during the latter stages of the test the specimen underwent two thermal cycles (power failures) which resulted in some loss of corrosion product and sudden irregular drops in temperature along the length of the specimen. Examination revealed localized attack in the form of void formation to a depth of several mils.

In another test with an X8001 specimen, both the heat flux and the coolant temperature were gradually decreased during the run in a manner similar to that expected in an ATR cycle (data supplied by Babcock and Wilcox personnel). Although examination of the specimen is incomplete, the temperatures measured indicate that the rate of oxide formation was lower than would have been predicted from an extrapolation of the results obtained in the HFIR corrosion program. A test identical to this, except that the specimen is 6061 aluminum, is in progress.

High Flux Isotope Reactor Design and Development

Physics. — HFIR critical experiments have thus far yielded a considerable amount of data for the clean core condition. These data can be compared with calculational results to provide a comparison between the nuclear physics of the experimental core (a reasonable material and dimensional facsimile of the design core) and that of the design core.

The first test performed was a check on neutron multiplication with the core submerged in water; the core was slightly subcritical ($k \cong 0.98$). Calculations predicted $k = 0.98 \pm 0.02$.

The next experiment was a check on the position of the control plates for a clean core; the height of the gray window (distance between the two gray-black interfaces) was determined to be 10.5 and 13.4 in., respectively, for the clean core with and without the target in the island. Corresponding calculated values, with corrections made for small differences

between the calculated and the experimental core (calculations were made before the experimental core was constructed), were 11 and 14 in. The minimum acceptable height of the gray window, based on power distribution and burnup of the black-rod ends, is approximately 6 in.

Of the above two tests the first was the better check on fuel loading, since the second test involved the reactivity worth of both the fuel and the control plates. Further tests concerning the worth of the fuel are to be conducted.

One of the more important functions of the present series of tests was to determine the power distribution obtained with the fuel distribution specified for the critical experiment, and to obtain information needed for making possible necessary changes in the fuel distribution. Experiments on the clean, critical core showed that the radial power distribution in the inner annulus was about 18% low at the inner edge and about 27% high at the outer edge, necessitating future minor changes in the fuel distribution. The distribution in the outer annulus was more nearly that desired. In the longitudinal direction the power distribution was satisfactory.

Information was obtained for estimating the peak thermal flux in the island. By use of a uranium foil in the island, calculational results to supplement the experimental power distribution data, and empirical relations to correct for the island-foil flux perturbation, a peak thermal flux of about 5.8×10^{13} nv/Mw was obtained. With a gold foil in the island and radiochemical analysis of two fuel plates to determine the power level of the experiment, a corresponding thermal flux of about 4.9×10^{13} nv/Mw was obtained. The calculated value was 5.5×10^{13} nv/Mw.

Interpretation of experimental reactivity measurements requires that the ratios of effective delayed-neutron fractions and effective prompt-neutron lifetimes, as well as the absolute values of effective delayed-neutron fractions, be known for the different core conditions. Average effective delayed-neutron fractions for the white, gray, and black control-plate positions have been calculated to be 0.00714, 0.00704, and 0.00629 respectively. The ratios of neutron lifetimes for white to gray and gray to black were calculated to be approximately 2 and 1.09 respectively.

Measurements of the temperature coefficients were made with all regions at the same temperature and with all regions except the fuel region at the same temperature. The calculated and experimental over-all and fuel-region coefficients with and without the target in the island are compared below:

HFIR Temperature Coefficients ($°F^{-1}$)

Temp (°F)	Calculated, Without Target		Experimental			
			Without Target		With Target	
	Over-all	Fuel	Over-all	Fuel	Over-all	Fuel
	$\times 10^{-4}$	$\times 10^{-4}$	$\times 10^{-4}$	$\times 10^{-4}$	$\times 10^{-4}$	$\times 10^{-4}$
70	+0.8	−0.8	+0.3	−0.5	−0.13	−0.5
	Δk_{max} = 0.002 (120°F)		Δk_{max} = 0.001 (120°F)			
150	−1.0	−2.0	−0.2	−1.1	−0.32	−1.1

Void coefficients of reactivity were also measured with and without the target in the island; calculated and experimental values of maximum Δk associated with island voids are listed below:

	With Target		Without Target	
	Δk	% Void	Δk	% Void
Calculated	+0.015	40	+0.025	45
Experimental	+0.015	40	+0.031	70

Experimental determination of control-rod worth and consideration of the tentatively defined operating and scram conditions for the HFIR indicate that the present control system is deficient by about 2% in reactivity. Possible remedies being considered include the addition of more burnable poison in the fuel and/or the use of different materials for the control plates.

Control and Instrumentation. — Elementary diagrams of the nuclear control system were completed and were submitted to the architect-engineers to permit them to begin the interconnection wiring diagrams.

Performance tests are nearing completion on the gas-filled temperature sensors and the heat-power calculator.

An analog study of the primary-loop pressure control system was completed.

Metallurgy. — An HFIR flow-test element is being fabricated as a prototype fuel element; the fabrication procedures wherever possible are those considered suitable for manufacture of the production units.

The uranium homogeneity in outer-annulus fuel plates, which contain a 23.90 wt % U–Al alloy core, has been studied. Air-melted slab castings have been made in which the uranium concentration was controlled to within ±1% of the average value.

Rolling of the majority of the fuel plates for the outer annulus was completed. Occasional difficulty was experienced with blistering, however.

The inner-annulus cores contain a dispersion of U_3O_8 in aluminum. Pronounced blistering has been observed during the rolling of these plates. Approximately 50% of the plates rolled to date are generally acceptable, however, indicating that the difficulty may be resolved by quality control.

In addition to the flow-test element, a mockup of prototype dimensions is being fabricated, by using unfueled plates of 6061 aluminum. The purpose of this unit is to study forming and assembly problems. Marked progress has been made in the forming and assembling of the outer annulus of this mockup. Measurements of 60 random spacings of the mechanically fixed plates revealed that all met specifications. Similar encouraging results were also obtained when the last five plates were welded to the tubular side plate by a series of short circumferential-type plug welds.

Design. — Detail drawings of the reactor core support components were completed and were issued for procurement for the HFIR hydraulic

mockup. Material and welding specifications for these mockup components were written for use in their procurement. Detail drawings and preliminary material specifications for the beryllium reflector were completed for use in prebid discussions with prospective vendors.

An experimental program was initiated to determine the hydraulic load distribution on the control rods. The effect of drilling holes in the plate to reduce the pressure differential is being experimentally determined. Control-rod load distributions will be used on an HFIR outer control rod to determine experimentally the stresses and deflections in long cylindrical segments under radial loads. A solid nickel cylindrical segment, 1/4 in. thick, is used as a reference.

Calculations based on current HFIR design indicate a maximum hot-spot oxide-water surface temperature of 344°F at a heat flux of 1.52×10^6 Btu hr^{-1} ft^{-2}. Buildup of oxide film over a 15-day operating period at this heat flux will result in a 576°F maximum metal surface temperature. Calculations have shown that at 100 Mw with a 900-psi nominal inlet pressure a 50-mil-diam blister in the 10-mil-thick meat portion of the fuel plate can raise the hot-spot heat flux to one-half the calculated burnout value. An investigation of the effect of local fuel-segregation area size and degree of segregation indicates that a 5% increase in local heat flux will result from an increase in fuel concentration of 20% over a 58-mil-diam area, or from a 10% concentration increase over a 111-mil-diam area.

Design of the control-rod-drive position indication equipment was completed. Designs of the N^{16} thimbles and the fission chamber thimbles are being reviewed.

Critical Experiments. — The reactivities of various configurations of the control plates of HFIR critical experiment No. 2 were measured by using the pulsed-neutron technique, although the results have not been corrected for changes in neutron lifetime and in effective delayed-neutron fraction with control-plate position. The uncorrected reactivity associated with full insertion of the outer control plate from the critical position (which was with 4.6 in. of the black section inserted) was −$4.7 and is to be compared to the value of −$4.9 obtained by integration under the control-plate sensitivity curve obtained during void coefficient measurements.

Boric acid has been added to the water that fills the space between the plates of the fuel element so that the aluminum or white sections of the control plates are adjacent to the core at critical. More control-plate calibrations are in progress using the pulsed-neutron method; however, for some of the configurations several exponentials are found in the neutron decay. The analysis to get the fundamental decay constant with confidence is difficult.

Additional power and flux distributions were measured when the boric acid concentration was sufficient to have the control plates form a white window of 10.8 in. at critical; that is, each gray section of the control plates was inserted 4.1 in.

NUCLEAR TECHNOLOGY AND GENERAL SUPPORT

Nondestructive Test Development. — An extensive study was made of low-voltage radiographic conditions to determine optimum techniques and the capabilities and limitations of such radiography for thin sections of aluminum, steel, and beryllium. The conditions varied during this program were the input kilovoltage (energy of the x-ray beam), the specimen thickness, and the intermediate atmosphere between the x-ray tube head and the specimen. The specimen thicknesses ranged up to approx 1/2 in. of aluminum, 2 in. of beryllium, and 0.037 in. of steel. Considerable advantage has been realized for both sensitivity and required exposure times through the use of intermediate helium atmospheres and darkroom, bare-film exposure techniques. Contrast sensitivities as low as 0.1% have been obtained, which is far superior to the normal practice of 2% sensitivity. A number of exposure technique charts were constructed as aids to optimum radiography.

Numerous empirical applications have been made of this system for the examination of aluminum, beryllium, graphite, steel, ceramics, epoxy compacts, and combinations of these and other materials. The configurations have included tubing, fuel capsules, plates, rods, cylinders, and other more complex shapes. Most of these items could not have been adequately inspected previously.

Mechanical Properties Research. — Zircaloy-2 tubing has been tested to determine an analytical model to describe the mechanical anisotropy and to determine the effect of radiation upon the creep-rupture life. It was shown previously that the fracture characteristics can be described fairly well by the relationship

$$F(S_t - S_r)^2 + G(S_u - S_r)^2 + H(S_u - S_t)^2 = 1 ,$$

where

S_t = tangential stress,
S_r = radial stress,
S_u = axial stress,
F, H, and G = anisotropy constants.

In performing the analysis on tubing tested at room temperature, the yield strength, fracture stresses, and the deformation ratios are described very well by the following constants: $H/F = 1$, and $G/H = 3.7$.

Preliminary creep-rupture results under varying stress ratios indicate that these same constants are applicable in describing creep-rupture properties at 700 and 900°F under tension-tension stress states.

Solid Reaction Studies. — Diffusion coefficients for the diffusion of columbium in reactor-grade, hafnium-free, iodide zirconium were determined in the temperature range 900 to 1500°C, wherein the body-centered-cubic β phase of zirconium is stable. Columbium-95 (35-day, 0.76-Mev gamma) was applied dropwise in the form of an oxalate solution to polished surfaces of specimens and evaporated *in situ* to deposit a thin residue of columbium oxalate. During diffusion annealing the oxalate decomposed to a columbium oxide, from which columbium diffused into the zirconium. Conventional techniques of sectioning and gamma counting were used to determine the columbium distribution in the specimen. The appropriate solution

of Fick's law for diffusion from a plane source into a relatively thick medium was used to calculate a diffusion coefficient at each annealing temperature. The pre-exponential factor, D_0, and activation energy, Q, in the Arrhenius equation $D = D_0 \exp(-Q/RT)$ were then calculated from a plot of diffusion coefficient vs the reciprocal of the absolute temperature. The temperature dependence of diffusion of columbium in zirconium in the temperature range 900 to 1500°C is represented by the equation $D = 2.06 \times 10^{-4} \exp(-32{,}700/RT)$ cm^2/sec.

Fuel Element Development. — The postirradiation examination of various aluminum-clad fuel plates containing U_3O_8, UC_2, and UAl_3 dispersed in aluminum, developed in connection with the Foreign Reactor Fuel Program, has been essentially completed. Although the visual examination of samples containing 20%-enriched 48 wt % U—3 wt % Si—bal Al and 65 wt % U_3O_8—bal Al irradiated at low temperatures to burnups as high as 6.6 and 5.7×10^{20} fissions/cc, respectively, showed no adverse effects of the irradiation, the hot-cell examinations revealed that reactions and dimensional changes were encountered at the high fuel burnups. Dimensional and density measurements on the oxide-bearing plates indicate that under irradiation, core shrinkage occurred which did not increase with burnup, whereas in the alloy-bearing plates a core swelling occurred which increased with fuel burnup. Similar measurements indicated that core swelling occurred in the UC_2-bearing plates, but insufficient data are available to correlate the swelling with burnup.

Metallographic examination of these irradiated samples indicates that microstructural changes had occurred as a function of irradiation. Numerous pores were noted in the U_3O_8 and UC_2 particles irradiated to high burnups, as well as the presence of reaction zones. Reaction zones were also noted around the UAl_3 particles in the alloy specimens, which increased as the irradiation progressed. In general, these various reaction zones appear similar to those observed in unirradiated specimens but treated at elevated temperatures. In spite of these reactions, it appears that either the alloy or the oxide dispersion is capable of being used in aluminum-base fuel elements operating at moderate temperatures and aimed at high fuel burnup.

Reactor Controls Development. — A neutron flux measurement apparatus was developed which is suitable for use in a variety of reactor configurations as part of the counting-rate instrumentation. The apparatus comprises a fission chamber, a preamplifier, and a drive mechanism. The movable assembly, which has a maximum outside diameter of 0.760 in., was made flexible so that a guide tube, curved as required, can be installed in the reactor shielding leading to the core. The assembly is waterproof and is designed to operate continuously in an ambient temperature of 100°C.

A prototype assembly was tested successfully in a new guide tube installed at the ORR. The integral counting rate decreased less than 10% when the pulse-height discrimination level was changed from a value equal to the alpha-particle pulse height (0.1 alpha count/sec) to twice this value. Tests in a gamma-ray field of 2×10^6 r/hr showed that the pulse pileup due to gamma rays was no greater than twice the alpha-particle pulse height.

The fission chamber contains concentric cylindrical electrodes coated with 1 mg/cm^2 of U^{235} over ~30 cm^2. The chamber is well saturated with 150 v applied; the operating polarizing voltage is 270 v. The collection time is 0.08 μsec. The special cable connecting the chamber and the preamplifier is designed to withstand a gamma-ray dose of 10^{10} r. The preamplifier, 0.760 in. OD and 12 in. long, contains two feedback amplifier sections. Subminiature vacuum tubes are used because of their resistance to radiation damage; each component of the preamplifier will withstand a gamma-ray dose of 10^8 r. The radiation dosage specifications are based on one year of continuous operation in high-flux reactors.

The preamplifier input stage is a two-tube, charge-sensitive feedback pair; the sensitivity changes less than 3% for variations in chamber capacitance from 0 to 100 picofarads. The output stage of the preamplifier is a three-tube feedback amplifier which drives a long balanced line terminated in its characteristic impedance by a loaded pulse transformer. The over-all gain of the preamplifier is 3×10^{12} v/coulomb. The output pulse height is 150 mv for a nominal 50-Mev fission fragment and 15 mv for a U^{235} alpha particle. The measured electrical noise is ≈5 mv peak-to-peak, and alpha particles are thus detectable with good signal-to-noise ratio. The system rise time is 0.15 μsec. The second differentiation in the pulse transformer gives an output wave form that is not subject to shifts in discrimination level due to changes in counting rate.

The movable assembly is driven by either a permanent-magnet dc motor or a two-phase ac induction motor, for use in the wide-range counting channel ("servo fission chamber") described in Trans. Am. Nuclear Soc. 3, 454 (1960). It is thus a part of the "second generation" of ORNL reactor instrumentation now under development.

Power Reactor Fuel Processing: Solvent Extraction. — In a preliminary test with short-decayed irradiated thoria fuel, all the thorium and uranium and 85% of the protactinium were extracted from a nitrate fuel solution. Decontamination factors were 4×10^4 from rare earths, 1.4×10^3 from ruthenium, and 100 from gross gammas in the first extraction cycle. If these results are typical, it will be possible to process 90-day-decayed Consolidated Edison thorium reactor fuel with an anticipated recovery of 99.9% of the fissionable and fertile material and remove >90% of the high-neutron-capture fission products.

About 90% of the protactinium was removed from a solution containing 2×10^5 counts min^{-1} ml^{-1} of Pa, 220 g per liter of Th, 15 g per liter of U, 0.09 M Al, 0.04 M F, and 9 to 10 M HNO_3 by adsorption on crushed unfired Vycor glass. About 59, 61, and 67%, respectively, of the protactinium was adsorbed on 0.5, 1, and 2 g of glass stirred with 50 ml of the solution for 15 min. A column packed with fired Vycor did not remove protactinium from the solution.

The use of tertiary amines as a plutonium extractant is being studied. After plutonium has been partitioned from uranium with trilaurylamine, it is stripped with acetic acid, which also extracts some nitric acid. In corrosion tests, type 347 stainless steel tubing suffered what appeared to be a mild etch when exposed 96 hr to 1 M HNO_3–2 M acetic acid–45 g per liter of $UO_2(NO_3)_2 \cdot 6H_2O$. Over-all corrosion rates were 0.02 mil/month.

Power Reactor Fuel Processing: Zirconium-Containing Fuel. – Engineering-scale studies on continuous dissolution of simulated highly enriched U-Zr alloy fuels in 6.5 M NH_4F–0.6 to 1.0 M NH_4NO_3–0.1 M H_2O_2 (modified Zirflex) were continued in 6-in.-diam equipment. The process system achieves stability and is easily controlled. Steady-state operation was satisfactory, and at a feed/fuel-element-surface ratio of 0.08 cm/min, the reaction rate was 5.6 mg cm^{-2} min^{-1} and the zirconium concentration 70 g/liter. When the feed/surface ratio was decreased to 0.06, the zirconium loading increased to 75 g/liter, but the product rate was lower because of a decrease in the reaction rate to 4.5 mg cm^{-2} min^{-1}. Dissolution rates were only slightly affected by removal or reflux of the reaction product NH_3 as NH_4OH.

Dissolution of zirconium in titanium equipment possibly can be accomplished by 3 M HNO_3–0.4 M HBF_4–1.2 M HF–0.46 M $(NH_4)_2Cr_2O_7$. Although in laboratory tests titanium was corroded at 1 in./month in this refluxing dissolvent, the very high initial corrosion rate decreased very rapidly as zirconium dissolved. At an F/Zr solution mole ratio of 26 with the titanium touching the dissolving Zircaloy-2, the alloy dissolved at 30 mg cm^{-2} min^{-1} and titanium corrosion was not measurable in short-term tests. Without coupling to Zircaloy-2, the titanium corrosion rate was also negligible at an F/Zr ratio of 9, and the Zircaloy-2 dissolved at a rate >20 mg cm^{-2} min^{-1}. The dissolver product was stable both at the boiling point and at room temperature when the zirconium concentration was 0.47 M Zr at a final F/Zr ratio of 6 and when the solution contained aluminum nitrate in equimolar amounts with the free fluoride, that is, all fluoride in excess of 4 moles per mole of zirconium.

Power Reactor Fuel Processing: Uranium-Graphite and Uranium Carbide Fuels. – Leaching of graphite–8% UO_2 fuel specimens for 4 hr with boiling 90% HNO_3 showed that the uranium recovery was affected only slightly by the terminal uranium concentration. Recoveries increased from 98.2 to 99.2% as the terminal uranium concentration in the leach solution decreased from about 50 to 10 g/liter.

Pebble-Bed Reactor prototype fuel spheres coated with SiC and containing UO_2-impregnated graphite were mechanically cracked and treated with boiling 90% HNO_3 at 60°C. After 3.7 hr of exposure, 60% of the fuel was disintegrated to less than 4 mesh. Uranium loss after washing was ~6%. The 30-mil SiC coating material was uniformly distributed among the sieve fractions; residual uranium concentration was higher in the 100/325 mesh fraction than in the +100 mesh material.

Uranium monocarbide containing about 17 mole % uranium metal reacted with water at 80°C to produce an average of 1.71 millimoles of H_2, 2.83 millimoles of methane, 0.48 millimole of carbon, and 1.29 millimoles of monatomic hydrogen as saturated C_2 to C_6 aliphatic hydrocarbons per gram of sample hydrolyzed. The off-gas contained 36% H_2 and 60% CH_4. The original specimen contained 4.03 millimoles of uranium and 3.33 millimoles of carbon by both synthesis and chemical analysis. These data indicate that the principal reactions occurring in the hydrolysis of U-UC mixtures are:

$$U + 2H_2O \rightarrow 2H_2 + UO_2 \cdot xH_2O \ ,$$

$$UC + 2H_2O \rightarrow CH_4 + UO_2 \cdot yH_2O \ ,$$

where the degree of hydration of the UO_2 is unknown.

Power Reactor Fuel Processing: Mechanical. – Nine NaK-bonded SRE core I fuel clusters, containing 668 kg of uranium, were successfully dejacketed mechanically. A total of 1624 kg of uranium has now been dejacketed, and only ~200 kg of the SRE fuel remains to be processed. The experimental production rate was ~6.0 kg of U per hour; about three times this rate would be expected from actual assembly-line processing with the present equipment. Analysis of NaK eutectic bond indicated a Cs^{137} concentration of 2×10^7 to 2×10^8 dis min^{-1} ml^{-1}.

In operability tests with the 250-ton prototype fuel shear, performance was generally satisfactory; however, minor modifications planned to optimize operations include improving the operation of the feed mechanism and fuel-assembly length indicator, changing the rubber gag inserts, and remachining the inner gag to facilitate easier removal from the shear.

Power Reactor Fuel Processing: Beryllium- and BeO-Containing Fuels. – GCRE fuel pellets (70% UO_2–30% BeO) were completely dissolved in 10 to 14 hr in boiling 8 M HNO_3 containing 0.5–0.8 M NaF. With no fluoride in the dissolvent, complete dissolution required at least 30 hr. The final solutions contained about 4 g of uranium per liter.

PHYSICAL RESEARCH PROGRAM

Reactor Operations. — Because an additional failure occurred in one of the ball-latch mechanisms of the ORR shim rod, the whole mechanism is being redesigned. Work is being continued on the boiling detecting device in the ORR. Preliminary tests on an acoustical monitor were not promising, and the reactor neutron noise method is now being evaluated.

The second annealing of the ORNL Graphite Reactor was completed on September 16 and 17. High temperatures were obtained in all regions of the reactor except for a small strip at the edges in the corners.

Waste Disposal. — A further reduction in the radioactive wastes discharged into White Oak Creek has been achieved by allowing the effluent from the Waste Treatment Plant to pass through the settling basin, where solid materials settle before discharge into the creek. It appears that this may have reduced the effluent by as much as 50%. Approximately half the strontium released in recent months has come from Melton Branch and, presumably, from the HRT.

Hot-Cell Operations. — A regular evening shift is now being worked in the 3025 hot cells; operations will be more effective when more personnel are available.

Dejacketing of fuel elements in the 3026D hot cells is almost complete.

PHYSICS AND MATHEMATICS RESEARCH

Charge Spectrometry. — By means of a mass spectrometer described previously [Phys. Rev. 107, 740 (1957)], measurements have been made on the distribution of charge fragments produced following the decay of CH_3I^{131}. A listing of the relative abundance of the different ions is as follows:

Ion	Relative Abundance
CH_3Xe^+	100.0
CH_3Xe^{2+}	0.04
CH_3^+	2.8
CH_2^+	3.5
CH^+	3.2
C^+	2.7
C^{2+}	0.1
H^+	2.0
Xe^+ to Xe^{16+}	29.5

The most striking observation is the large amount of CH_3Xe^+, for in a similar study on CH_3T it was found that after β^- decay the C-He bond

rarely remained intact, in spite of the fact that the recoil energy and other modes of excitation should be less for CH_3T than for CH_3I^{131}.

Neutron Diffraction. – In order to account for the magnetic properties of alloys it becomes important to determine the individual magnetic moments of the constituent atoms. This determination can be accomplished by the combination of neutron diffraction and magnetic induction measurements. Such measurements were made on the following ferromagnetic alloys: Pd_3Fe, PdFe, Pd_3Co, PdCo, Ni_3Co, and NiCo. The average moment values were obtained from magnetic induction measurements, while the differences in the atomic moments were determined from either the ferromagnetic diffuse scattering of the disordered alloys or the superlattice reflections of the ordered alloys. In some cases, short-range-order effects were observed, and these complicated the interpretation of the results.

Fast-Chopper Time-of-Flight Spectrometer. – Transmission measurements on a 50-g sample of Pa^{231} have been made at low neutron energies, using an energy resolution of ~1.5% with a 45-m flight path. Measurements have been extended to 200 ev with an energy resolution of 0.2%, using the 180-m flight path. A shape analysis has been made on the first seven resonances up to 3.5 ev; this resulted in radiation widths which vary from 38 to 47 mv. An area analysis has been made on the resonances up to 75 ev, which resulted in a value of 1.0 ev for the average level spacing per spin state and a value of 0.9×10^{-4} for the s-wave strength function.

High-Voltage Experimental Program: Coulomb Excitation of Osmium and Chromium Nuclei. – Coulomb excitation measurements have been made by alpha-particle bombardment of metallic targets enriched in the different isotopes of osmium and chromium. Some of the results are summarized below:

Nucleus	Energy (kev)	$B(E2)_{ex}$ (cm^4)	$T_{1/2}$ (sec)
Os^{192}	206	$(2.34 \pm 0.23) \times 10^{-48}$	$(2.49 \pm 0.25) \times 10^{-10}$
Os^{190}	187	$(2.72 \pm 0.27) \times 10^{-48}$	$(3.16 \pm 0.32) \times 10^{-10}$
Os^{188}	155	$(3.19 \pm 0.32) \times 10^{-48}$	$(5.36 \pm 0.54) \times 10^{-10}$
Cr^{50}	782 ± 8	$(1.15 \pm 0.08) \times 10^{-49}$	$(8.4 \pm 0.7) \times 10^{-12}$
Cr^{52}	1433	$(7.3 \pm 0.7) \times 10^{-50}$	$(6.4 \pm 0.7) \times 10^{-13}$
Cr^{53}	565 ± 6	$(1.18 \pm 0.08) \times 10^{-50}$	
Cr^{54}	838	$(1.06 \pm 0.07) \times 10^{-49}$	$(6.4 \pm 0.5) \times 10^{-12}$

The $B(E2)_{ex}$ for the first 2^+ state of Os^{190} is 60% higher than the value derived from Sunyar's lifetime measurement (Proc. U.N. Intern. Conf. Peaceful Uses Atomic Energy, 2nd, Geneva, 1958, paper 646). Lemburg's value (Reactions Between Complex Nuclei, Wiley, New York, 1960, p 112) of $B(E2)_{ex}$ for the first 2^+ state of Cr^{54} is about a factor of 2 lower than the value obtained here. The other values of $B(E2)_{ex}$ for 2^+ states listed above

agree reasonably well with other published information. In particular, there is good agreement for Cr^{52} with the resonance fluorescence result of Ofer and Schwarzschild [Phys. Rev. Letters 3, 384 (1959)]. Two states in Os^{189} at 69 and 219 kev are directly Coulomb-excited. Angular distribution measurements lead to a unique spin assignment of 7/2 for the 219-kev state. The 30-kev isomeric state in Os^{189} is found to be indirectly excited via the 219-kev state.

High-Voltage Experimental Program: The $C^{13}(He^3,n)O^{15}$ Reaction. — Pulsed-beam time-of-flight techniques with time resolution capabilities of 4 mμsec for neutrons have been used to study neutrons from the ground state and the third excited state (6.15 Mev) for the reaction $C^{13}(He^3,n)O^{15}$. Excitation functions were measured at 0 and 90° for He^3 energies from 1 to 2.7 Mev. Angular distributions were measured at an He^3 energy of 2.66 Mev. The IBM 7090 distorted-wave code of Satchler et al. [Bull. Am. Phys. Soc. 6, 66 (1961)] was used to fit these angular distributions. Tentative fits show $\ell = 0$ for the ground state and $\ell = 3$ for the third excited state. From these transfers, preliminary assignments of $(1/2^-)$ for the ground state and $(5/2^+ \rightarrow 7/2^+)$ for the third excited state have been made.

CHEMISTRY RESEARCH

Effects of Radiation on Analytical Methods. — A study has been initiated for the purpose of evaluating the effects of radiation on methods of chemical analysis. A source of gamma radiation, Co^{60}, was calibrated. Fluxes up to approximately 5000 r/hr — the range normally encountered by the analyst working with radioactive samples — are available from this particular source unit. Ethylenediaminetetraacetic acid was selected as the first reagent for study because of its widespread use in analytical chemistry.

Spectrophotometric Studies of Solutions at Elevated Temperatures and Pressures. — A spectrophotometer system based on the Cary model 14 spectrophotometer was designed by the Applied Physics Corporation to ORNL specifications for operation up to the critical temperature of water and for pressures up to 10,000 psi. A complete cell was fabricated, and extensive tests showed it to be entirely satisfactory for operation up to at least 330°C and 3000 psi. Special features of the system include an automatic digital data readout on IBM cards (or perhaps magnetic tape), a viewing port and mirror for visual observation of the test solution at all operating temperatures, and a vertical slit system for spectral measurements on individual phases of two-phase systems by individual adjustment of the slits. A system for rocking the cells at variable speeds while they are operating at elevated temperature and pressure was designed to permit mixing of the cell contents and equilibration of the gas in the cell over-space with liquid and to remove bubbles that may form on the cell windows. Part I of a report on the problem of the Cerenkov radiation in making spectrophotometric measurements on highly radioactive solutions was issued as ORNL-3180.

A miniature loop system operable up to 150°C and 200 psi for circulating solutions through special cells in a standard Cary model 14 spectrophotometer was designed and constructed by ORNL and set up for preliminary

testing external to the spectrophotometer system. It can be used in the standard Cary model 14 spectrophotometer system without modification of the spectrophotometer. The auxiliary system for digital output from the wavelength and absorbancy information includes circuitry that prevents output of spectral data while the recorder (single pen) is changing between ranges of absorbancy and a photoelectric pulse generator for digitizing the wavelength information.

Volatility Studies. – In a revised system for removing entrained fused salt, nickel, and oxides from the hydrofluorinator discharge gas stream installed in the Pilot Plant, the recirculating HF is scrubbed by a condensing fraction of the HF. Tests indicated that the flash cooler is adequately designed and that the scrubbing system performs satisfactorily. In two runs there was no line plugging with solids, and a metal-wool filter in the gas stream showed no increase in pressure drop due to solids.

The applicability of the fused salt–HF dissolution system for fuel materials other than zirconium is being explored systematically. Massive zirconia plates were dissolved by HF in molten $NaF-LiF-ZrF_4$ at 1.24 and 3.13 mg cm^{-2} min^{-1} with HF rates of 1.9 and 11.3 g/min. The variation in dissolution rates with changing HF flow rate is the same as for zirconium metal. However, it is encouraging that at any given HF mass flow rate the dissolution rate of this oxide is several times that of zirconium. A type 304 stainless steel tube containing eutectic Na-K was dissolved by HF in fused salt at a wall penetration rate of 2 mils/hr.

Uranium was recovered from Zircaloy-2–clad UO_2 fuel pins, irradiated to 600–1200 Mwd/ton and decayed 14 to 28 days, by dissolution in 24-31-45 mole % $NaF-LiF-ZrF_4$ at 650°C with HF at a rate of 10 mg cm^{-2} min^{-1} and fluorination of the melt at 500°C. The chief activity in the UF_6 product of five tests can be attributed to U^{237} and a negligible amount of Mo^{99}. The other short-half-life fission products of interest in these tests were I^{131}, Te^{127}, Te^{129}, and Te^{132}. The IF_7 and TeF_6 presumably formed in the fluorination step were separated from the UF_6 in the absorption step, indicating no complexing of these materials with NaF.

In additional studies on the mechanism of the absorption of UF_6 by NaF pellets, partial differential equations were derived for the concentration of unreacted UF_6 as a function of time and position in a sphere of NaF. The model includes the effects of stagnant gas film, resistance, diffusion rate of UF_6 in the pores of the sphere, reaction rate at the pore walls, and local UF_6 loading on the rate of transport and of reaction at the surface. The equations were converted to finite difference form in preparation for numerical solution, to be followed by experimental checks of the model.

Solvent Extraction Research. – Monoalkylbenzenes showed promise as diluents with improved chemical stability for use with organophosphorus extraction reagents, for example, tributyl phosphate. In an extraction test where lower $Zr-Nb^{95}$ extraction coefficients indicate greater stability, a 1 M TBP solution in n-butylbenzene had an extraction coefficient 1/200 of that of 1 M TBP in Amsco 125-82 after both solutions had been exposed to boiling 2 M HNO_3.

Keto-oximes added to aqueous feed solutions improve separation of uranium from Zr-Nb and Ru in TBP extraction. In batch countercurrent

extractions with 1 M TBP—Amsco 125-82 from Zr-Nb^{95} tracer solutions, Zr-Nb extraction was a factor of 170 lower with 0.1 M diacetone alcohol and 0.1 M sodium nitrite in the feed. The system is assumed to yield a keto-oxime by the reaction

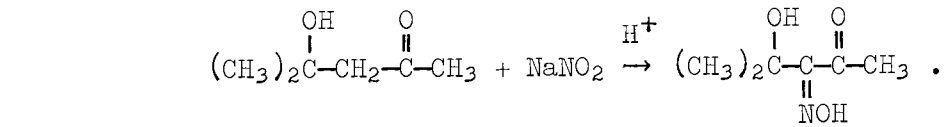

A chemical flowsheet was proposed for final-cycle plutonium purification by tertiary amine extraction (ORNL-3048) and acetic acid stripping (ORNL-3074). A Purex partitioning-cycle plutonium stream can be accepted as feed with no adjustment other than re-oxidation of plutonium to Pu(IV); sulfate can be tolerated at the levels expected from ferrous sulfamate reductive stripping in the Purex cycle.

Isotherms for extraction with trilaurylamine (TLA) in diethylbenzene from 1.5 M HNO_3, fitted by the empirical equation

$$E_a^o(Pu) \approx E_1[\underline{M}_{amine} - 3\,\underline{M}_{Pu}]^2 ,$$

where E_1 is defined by $\log E_1 \approx 3.5 - 2.5\sqrt{\underline{M}_{SO_4}}$, were confirmed by batch countercurrent demonstration with 0.3 and 0.1 M TLA and simulated feed of 1 g of Pu per liter—1.5 M HNO_3—0.03 M $Fe(NH_2SO_3)_2$. The product solution contained 20 g of Pu per liter. Zirconium-niobium tracer in the feed (7×10^5 gammas min^{-1} ml^{-1}) could not be detected in a gamma scan of the product. Radiochemical analysis for zirconium in the product showed 116 Zr gammas min^{-1} ml^{-1}; the decontamination factor for Pu/Zr was 5×10^4.

Nuclear Methods of Chemical Analysis. — The determination of U^{235}, in materials containing uranium, by delayed-neutron counting was investigated to ascertain the suitability of this method for the routine determination of U^{235}. It was established that the method is excellent for routine application to the following types of analyses: (1) determination of total uranium in materials containing uranium of known isotopic composition, (2) determination of U^{235} in materials containing uranium of unknown isotopic composition, and (3) determination of the isotopic composition of uranium in materials containing known amounts of uranium.

In this study, samples were activated by exposure in the pneumatic-tube irradiation facility of the ORR, which provides a flux of about 6×10^{13} thermal neutrons cm^{-2} sec^{-1} when the reactor is operating at a power level of 30 Mw. After the samples were activated, a BF_3 counter assembly surrounded by a neutron moderator (paraffin) was used to measure the number of neutrons given off by each sample. The counting efficiency of this assembly is of the order of 5%. Under these conditions, 1 nanogram of U^{235} produced 10^3 counts during a 3-min counting period. This method, therefore, can be readily applied to the determination of from 0.001 to 10 μg of U^{235}. Since the particular facility used can accommmodate samples of from 1 to 6 g, depending on the density, the applicable concentration range is 1 ppb to 10 ppm of U^{235}.

Other elements which are fissioned by thermal neutrons, namely, U^{233} and Pu^{239}, were not present in any of the samples analyzed, so that interferences from these elements were not observed. Elements which become

sources of intense gamma radiation in the neutron radioactivation step of the procedure, for example, aluminum, interfere by gamma-ray "pileup" in the neutron detectors. This interference can, however, be eliminated by inserting lead shielding between the sample and the neutron detectors.

The relative standard deviation of this method is about 3%. This variability is believed to be due primarily to differences in the positioning of the sample in the neutron flux as the sample is successively removed from and returned to the irradiation facility.

Organic Chemistry. – The interactions in solution between compounds of the general type R_3PS and Ag(I) or Hg(II) were studied, since Handley and Dean [Anal. Chem. 32, 1878 (1960)] have shown $(RO)_3PS$ compounds to be selective solvents. The coordinating affinity of R_3PS for Ag(I) and Hg(II) varied with the electron-releasing properties of the R groups, that is,

$$C_4H_9- > C_6H_5- > C_4H_9O- > C_6H_5O- .$$

The following crystalline adducts were isolated in pure form:

$$(C_4H_9)_3PS\cdot AgNO_3,\ (C_4H_9)_3PS\cdot 2HgI_2,\ \text{and}\ 2(C_6H_5)_3PS\cdot AgNO_3.$$

The compound $(C_4H_9)_3PS\cdot AgNO_3$ was highly associated in benzene (seven times formula weight) according to cryoscopic measurement. The addition of more Bu_3PS reduced the degree of association. Infrared spectral measurements of the pure compound, in Nujol mulls, indicate that the nitrate is ionic rather than covalent.

Chemistry of the Heavy Elements. – The $DClO_4$-D_2O-H_2O system is a promising solvent for high-temperature aqueous spectrophotometry of inorganic ions. The transparency of the ClO_4^- anion throughout the wavelength range of interest (0.2 to 2.0 μ) plus its notable stability and weak association properties suggest it as an ideal reference medium. However, at elevated temperatures it is a powerful oxidizing agent, and the reduction products, HOCl and Cl_2, absorb in the spectral region below 0.5 μ.

Solutions of 0.01 and 0.10 M (25°C) $DClO_4$ have been examined spectrophotometrically for periods of 1 to 2 days at 250°C in a 3.81-cm cell of titanium, sapphire, Teflon, and gold. Decomposition rates < 20 ppm/hr for 0.01 M $DClO_4$ and 25 ppm/hr for 0.1 M $DClO_4$ were estimated from the growth of an absorption band at 0.310 μ due to chloroaurate(III) ($\epsilon_{Au} \sim 4200$).

The 0.01 and 0.10 M $DClO_4$ solutions will be re-examined after elimination of gold from the cell. These studies will be extended to higher perchlorate concentrations.

Radiation Chemistry. – Radiolytic decomposition of greater than 3 mole % of the alkali-metal bromates was accomplished with Co^{60} gamma rays. The amounts of bromate ion decomposed increased linearly with dose at first, but subsequently the dependence became nonlinear for all salts except $LiBrO_3$. The initial 100-ev radiolytic yields or G_0 values for bromate decomposition were: 0.31, 1.46, 1.71, 2.33, 3.4, and 5.1 for $LiBrO_3$, $NaBrO_3$, $KBrO_3$, $RbBrO_3$, $CsBrO_3$, and $TlBrO_3$ respectively. The yields increased only slightly with temperature between −195 and 85°C and, for $CsBrO_3$, were almost independent of the dose rate from 8.3×10^{20} to 7.1×10^{22} ev $mole^{-1}$ hr^{-1}.

The radiolysis of bromate ion gave bromite, hypobromite, bromide, and oxygen gas in amounts which varied with the alkali-metal cation in the salt and with the total dose absorbed. Virtually all the oxidizing fragments produced in the crystalline salts by irradiation could be removed by thermal annealing.

The radiolytic yields for bromate decomposition could not be correlated either with the thermodynamic stability of the salts or with their isothermal decomposition rates observed in the absence of radiation. However, an exponential dependence of G_0 on the crystal "free space" was found, and a mechanism for the decomposition of the molecular bromate ion could be proposed.

Electrochemical Kinetics and Its Application to Corrosion. — In a continued study of cathodic processes on passive zirconium, experiments were conducted to determine the reaction products of oxygen reduction. In most known electrode systems oxygen is reduced to hydrogen peroxide, considerable quantities of which can be found in solution under appropriate conditions. At low current densities on zirconium only about 10% or less of the theoretical amount of hydrogen peroxide was found in solution; at higher current densities, about 40% was found. Both the decomposition rates and the reduction rates of H_2O_2 were found to be negligible in the solutions studied. Only a minor pH effect was observed, but there was a slight tendency for increased acidity to increase the rate of reduction. These experiments, along with previously reported observations, suggest the following mechanism: (1) $O_2 + e^- = O_2^-$(adsorbed) (slow step); (2) O_2^-(adsorbed) $+ H^+ + e^- = HO_2^-$(adsorbed). The adsorbed HO_2^- ion is either desorbed to form hydrogen peroxide in solution or decomposed on the surface to form oxygen and water. The former process is favored at the more negative potentials (high-current-density region) and accounts for the larger amount of hydrogen peroxide found in solution.

High-Temperature Aqueous Solution Chemistry. — Experimental data for the critical temperatures of the two-component system SO_3-H_2O have been analyzed in terms of the van der Waals equation of state for binary systems. The temperature dependence of the van der Waals a for water was calculated from the data of Holser and Kennedy [Am. J. Sci. 257, 71 (1959)]; the a's for SO_3 and for interaction were assumed to have the same temperature coefficient. All the b's were treated as being temperature independent. With these refinements and a least-squares evaluation of two remaining interaction constants, an empirical equation was obtained which describes the experimental data over the entire concentration range with a standard error of estimate of 3.6°K. The temperature range covered starts from 647.3°K, the critical temperature of water, goes through a maximum of 945.2°K at $X_{SO_3} = 0.383$, and drops to 491.4°K for pure SO_3. The constants for the equation are:

for SO_3,

$$a_1 = 9.805 - 0.003257T ,$$

$$b_1 = 0.06029 ;$$

for H_2O,

$$a_2 = 7.574 - 0.003257T \quad \text{(Holser and Kennedy)},$$

$$b_2 = 0.03049 ;$$

interaction constants,

$$a_{12} = 24.6305 - 0.003257T ,$$

$$b_{12} = 0.06087 .$$

The final equation is

$$T_c = \frac{8(a_1X_1^2 + 2a_{12}X_1X_2 + a_2X_2^2)}{27R(b_1X_1^2 + 2b_{12}X_1X_2 + b_2X_2^2)} .$$

Physical Chemistry of Molten Salts: Cryoscopy in Fluoride Systems. — Measurements of the liquidus temperatures for the system LiF-NaF have now been extended to cover the entire concentration range. These measurements, which were of the precision ±1°C, permitted the evaluation of partial molal excess free energies of mixing for each component to a precision of ±8 cal. The free energies were found to be (1) negative in sign, (2) asymmetric with composition, (3) and otherwise inconsistent with regular solution behavior. Properties 2 and 3 are in disagreement with a recent theory of thermodynamic properties of ionic melts (Lumsden, Discussions of Faraday Society, 1961).

An empirical equation of the form $\Delta F^E = n_1N_2(a + bN_1)$ was used to rationalize the data. (ΔF^E = total excess free energy of mixing, n_1 = number of moles of LiF, N_1 and N_2 are the mole fractions of LiF and NaF respectively, a and b are constants with the dimensions of calories.) The excess partial molal free energies of mixing of LiF and NaF, respectively, are then given by the equations

$$\frac{\partial \Delta F^E}{\partial n_1} = aN_2^2 + 2bN_1N_2^2 , \qquad (1)$$

$$\frac{\partial \Delta F^E}{\partial n_2} = aN_1^2 + bN_1^2(N_1 - N_2) . \qquad (2)$$

The observed asymmetry in the partial free energies is accounted for in the second term in each of the above equations. The constants a and b, evaluated from the data in Eq. (1) (a = −820 cal, b = −310 cal), were used to calculate the free energies of NaF from Eq. (2). Up to concentrations of 50 mole % LiF these calculated values were equal to within ±8 cal of the experimentally derived partial molal free energies of mixing. At higher concentrations of LiF (from 50 to 60 mole %) the calculated values diverged markedly from the experimental quantities.

The constant a is believed to reflect changes, on mixing, of Coulombic repulsion, London dispersion forces between the cations, and the polarizability of the anion. The asymmetry constant b is believed to reflect changes in the interactions of third nearest neighbors.

Physical Chemistry of Molten Salts: Association in Nitrate Systems. — The association constants K_1, K_2, and K_{12} for the formation of AgBr, $AgBr_2^-$, and Ag_2Br^+ in molten $NaNO_3$ and in molten KNO_3 have been evaluated at several temperatures in the range 400 to 500°C. Within experimental error

the temperature dependence of these association constants was found to be consistent with the results of calculations based on the quasi-lattice model; K_1 for the formation of AgBr is larger in KNO_3 than in $NaNO_3$ (e.g., at 402°C, K_1 in mole fraction units is 932 in KNO_3 and 633 in $NaNO_3$). Most of the observed difference may be attributed to a Coulomb effect involving differences in the sizes of both of the cations and both of the anions in a given system.

Chemical Separation of Isotopes. — Selectivity coefficients for the reaction $Cs^+ + MR = CsR + M^+$, where M = Na or K, were measured in anhydrous ethylenediamine as a function of loading, resin cross linking, resin type, and eluting agent concentration. The concentration of the eluting solution in the range studied (< 0.2 M) had little effect on the selectivity coefficient. Some selectivity coefficients measured at 30°C for ~0.017 M eluting solutions are presented below:

Resin	Initial Form	Selectivity Coefficient
Dowex 50-X1	Sodium	7.6 ± 0.5
Dowex 50-X8	Sodium	18 ± 1
Dowex 50-X16	Sodium	79 ± 8
Dowex 50-X-1	Potassium	1.8 ± 0.2
Dowex 50-X8	Potassium	2.6 ± 0.3
Dowex 50-X16	Potassium	37 ± 0.4

The dependence of the selectivity coefficient on the composition of ethylenediamine-water mixtures was studied. Also measured was the swelling, in ethylenediamine, of various resins in different ionic forms.

Chemical Applications of Nuclear Explosions. — A number of solids that may be present in rock salt were tested as catalysts for vapor-phase exchange in the H_2-H_2O-HTO system. The measured values were compared with the equilibrium exchange that can be obtained with platinum as the catalyst for the same reaction. The chlorides were not very effective catalysts, while oxygenated salts and oxides in the form of large crystals were moderately effective:

Substance	Surface Area (m^2/g)	% of Equilibrium Exchange Achieved with Pt Catalyst
NaCl	0.015	0.65
$CaCl_2$	0.39	6–7
K_2SO_4	0.007	42.5
Silica gel	520	44
Al_2O_3	6.7	77
K_2CO_3	0.073	80
Drierite ($CaSO_4$)	9.7	95

The results are consistent with the view that exchange involves adsorption of one or all of the reactants on a surface containing exposed oxygen atoms. The chloride exchange is believed to involve reversible hydrolysis. Surface area differences apparently affect exchange in some cases.

Studies of the mechanism of the reduction of magnesium sulfate by hydrogen at 750 to 800°C indicated that the sulfate is first reduced to the sulfite, which thermally decomposes to MgO and SO_2 at the reduction temperature. Sulfur dioxide reacts very rapidly with hydrogen at these temperatures to produce H_2S, H_2O, and free S when catalyzed by the MgO. All steps in the proposed mechanism have been checked by direct experiment except formation of $MgSO_3$. Experiments at 650°C indicated that the decomposition is more rapid than the sulfate reduction, and thus the sulfite cannot be detected directly.

METALLURGY AND MATERIALS RESEARCH

Metallurgy of Superconducting Materials. — A research program has been initiated to determine the effects of metallurgical variables on the superconducting properties of superconducting metals, alloys, and intermetallic compounds. The present program is concerned with the systems Nb-Sn, Nb-Zr, Tc-Zr, and Tc-Mo.

Through the use of diffusion couples, at least three and probably four intermetallic compounds were detected in the Nb-Sn system. Only the single intermetallic compound Nb_3Sn has been previously reported by other workers. Wire made by filling an Nb tube with a mixture of Nb and Sn powder and fabricating to 0.015 in. OD was heated at 1000°C for 18 hr (the recommended heat treatment for best superconducting properties). This wire contained at least four Nb-Sn phases and a small amount of material which was liquid at the sintering temperature. A void content of between 25 and 50 vol % was also found.

The transformations of homogenized and quenched Nb-Zr alloys (25 to 50% Zr) were found to be extremely sluggish. These alloys are single phase above 1000°C and consist of two body-centered cubic phases between 610 and 1000°C, and of α-zirconium and niobium solid-solution phases below 610°C. The transformations of severely cold-worked alloys are being examined.

Arc melts of purified technetium were made, the largest weighing 28 g. Alloys of Tc-Zr and Tc-Mo were arc-cast in 10-g buttons. The critical temperature of purified technetium was found to be 8.22°K. The previously reported value of 11.2°K was determined on powdered metal which was probably seriously contaminated with oxygen. A glove-box metallographic facility was built and used for metallographic examination of technetium and its alloys. The recrystallization temperature of purified technetium cold-worked to about 90% reduction was found to be less than 800°C. The studies to date show that technetium seems to be similar to rhenium in the rate of work hardening and the very high hardnesses reached with a relatively small amount of cold working.

Ceramics Research: Sintering Studies. — Previously reported sintering-rate studies with thoria compacts showed that as the temperature is steadily increased, the densification rate increases to a maximum at about

1000°C, declines to a minimum at approx 1200°C, and increases again. Further tests with thoria calcined at higher temperatures before compacting indicated that decomposition or release of an impurity is not the cause of the minimum. A similar study of densification rate was made for two other materials having the fluorite structure. Densification rate curves on calcium fluoride and ceric oxide showed a minimum to occur at a temperature equivalent to approximately the same fraction of the absolute melting point as with thoria. The similar results with three substances having the fluorite structure suggest that the minimum is caused by an effect that is general for this lattice structure. It is possible that this may be caused by a change in mechanism of material transport. Materials having other crystal structures will be examined.

Physical Property Studies. — Thermal-conductivity measurements on 93.4% theoretically dense UO_2 in the radial heat flow apparatus have been extended to 527°C, where $k = 0.438$ w cm^{-1} $(°C)^{-1}$. The data are within ±2% of a smooth curve which agrees (within 3%) with the data of Howard and Gulvin (Thermal Conductivity Determination on UO_2 by a Radial Flow Method, IG Report-51, RD/C UKAEA, Culcheth, 1961).

Work has continued on establishing the calibration curve for the thermal comparator, which will measure the thermal conductivity of small specimens (1/4 in. thick by 1 in. in diameter). The problem of sphere flattening has been solved by replacement of the silver used for the detector spheres with an internally oxidized Ag-Mg alloy. The apparatus chamber has been altered such that specimens can be changed without loss of the protective atmosphere. The apparatus will give results reproducible to 3% for hard materials with conductivities less than iron; however, some further developments are necessary for soft materials of higher conductivity.

The temperature dependence of the total hemispherical emittance of platinum, matte- and bright-finished INOR-8, and several oxidized INOR-8 specimens was measured between 100 and 700°C. The method employed an instrumented strip specimen heated electrically in a black-body vacuum chamber held at a constant temperature. The results indicate that the total hemispherical emittance of INOR-8 at 600°C is increased threefold by a 1-hr oxidation at 1000°C. The total hemispherical emittance of bright-finished INOR-8 has a value of 0.24 at 600°C and was found to be sensitive to the original surface finish. The results on platinum agree with previously reported values.

CONTROLLED THERMONUCLEAR RESEARCH

DCX-1 Facility. — The fast electronic regulator designed to improve the stability of the 600-kv dc supply of DCX-1 was completed and tested. Comparison of performance shows a 150-msec rise time and 50% beam current ripple with the regulator off, and a 50-μsec rise time and 50% current ripple with the regulator on.

The onset times of the cyclotron radiation and two overtones were noted as functions of pressure and beam injection current. It is deduced from the data that the fundamental appears at a time corresponding to a density of 2.2×10^6 hot ions/cm^3, the first overtone at 4.8×10^6 hot

ions/cm^3, and the second at 9.8×10^6 hot ions/cm^3. Attempts are being made to interpret these findings in terms of the Harris instability theory and the negative-mass instability theory.

Slow ions escaping the plasma region through the magnetic mirrors have been energy-analyzed by a slow-ion spectrometer. The number of escaping ions increases rapidly at a pressure of 4 to 8×10^{-5} mm Hg for both argon and helium gas bleed. This increase is higher by a factor of 1000 than the rate of increase noted at lower pressures. Theory attributes such an increase to the ionization of neutral background gas by electrons. Other predictions of the theory are being pursued to complete the comparison. Radiation at the cyclotron frequency also has a sharp increase in intensity at the same pressure.

The addition of a bakeable liquid-nitrogen-trapped diffusion pump with a base pressure of 4×10^{-9} mm Hg to the liner region of the DCX was completed. A partial short in the east inboard coil has shifted the magnetic midplane and decreased the central magnetic field. The coil is being replaced. A break in the water jacket of a diffusion pump has necessitated the cleaning of the ion source and accelerator system.

High-Current Injection. — New electrodes were designed for the accelerator tube which have reduced the amount of voltage cleanup required to hold 600 kv. These electrodes should be more easily adapted for shielding the beam from the transverse magnetic field of the DCX-2 and will allow the incorporation of some x-ray shielding inside the tube.

The accelerator tube and the solenoid lens were moved from the test facility to the DCX-2, and preliminary tests of the new electrodes within the transverse magnetic field of the DCX-2 should begin during the first week of October.

Theory. — A new formula for the mode I—mode II transition in arcs, obtained by introducing effects of streaming to end walls into a method of Kadomtsev, predicts instability for magnetic fields higher than a critical value depending on ion and electron temperatures.

An attempt to obtain from a two-fluid magnetohydrodynamic approximation the plasma instability occurring when the electron plasma frequency exceeds any harmonics of the ion cyclotron frequency has yielded correct results for the lowest harmonics and for $\vec{k}$ nearly parallel to $\vec{B}$, but generally predicts greater stability.

The proof of the conjecture that all plasmas anisotropic in velocity are unstable if magnetic perturbations are admitted has been extended to more general classes of distributions.

Multigroup diffusion theory has been employed to calculate numerically the H^3 breeding ratio in a lithium-beryllium blanket bombarded by neutrons from a thermonuclear device. Breeding ratios as high as 1.45 were found.

Radio-Frequency Heating. — Studies are continuing on the plasma formed by heating electrons at the cyclotron frequency (3-cm, 0.75-kw microwave source) in a magnetic mirror configuration. Two distinct modes of operation are demonstrable: a low-pressure mode (5×10^{-6} mm Hg) in which the density ranges from 10^9 to 10^{10} and the electron temperature is greater than 0.1 Mev, and a high-pressure mode (10^{-5} mm Hg) in which the densities are greater than 10^{12} and electron temperatures are of the order of 5 kev. This plasma is very highly ionized, as evidenced by neutral-beam transmission experiments.

BIOLOGY AND MEDICINE PROGRAM

SOMATIC EFFECTS OF RADIATION

Pathology and Physiology: Recovery from Somatic Effects of Radiation. — Irradiated recipients of homologous mouse bone marrow cells in many donor-recipient combinations die of a wasting disease within 30 to 60 days after treatment. Such deaths have been attributed to immunological incompatibility between recipient and donor tissues; however, some recipients survive and retain the infused marrow for many months. The C57BL and 101 bone marrow cells that were grown for periods of 15 to 64 days in lethally irradiated (C57BL × 101)F_1 recipients were retransplanted into secondary F_1 recipients in an attempt to evaluate the immunological competence of the grafted cells over a period of time in which they should have been reacting against the host. When either type of parental marrow was allowed to grow in primary recipients less than 30 days and subsequently transplanted into secondary recipients, the survival of secondary recipients was inferior to that of primary recipients. However, when parental marrow remained in primary recipients more than 30 days, the survival of secondary recipients was superior to that of primary recipients. The erythrocytes in all the secondary recipients were of donor type. These effects may be ascribed to alterations of the immunological competence of the donor marrow rather than to its failure to take or to its rejection. These results are consistent with the idea that sensitization of the donor marrow may have occurred when the marrow was retransplanted within 30 days after the initial transfer, but immunological paralysis, exhaustion, partial tolerance, or mutual adaptation between donor cells and recipient may have occurred when the marrow was retransplanted after periods of 30 days or longer.

RADIATION GENETICS

Mutagen Mechanisms: Bacterial Genetics. — The genetic analysis of the factors determining radiation behavior was extended to include both ultraviolet (2537 A) and ionizing radiation. At least one of the genes involved in determining x-ray sensitivity is also involved in the determination of ultraviolet sensitivity. Preliminary data indicate that this gene may be located between the regions controlling histidine and proline synthesis. The technique for scoring radiation sensitivity of recombinants has been considerably improved, allowing the suggestion that two genes are involved in determining the difference in sensitivity to x irradiation observed for the HFr and F^- cultures being studied.

COMBATING DETRIMENTAL EFFECTS OF RADIATION

Mammalian Recovery: General. — Additional data are now available on the ability of white blood cells to prevent death of mice from the acute

radiation syndrome. Nine of ten mice exposed to 950 r and then injected with 35 to 40 million white blood cells are alive 45 days after irradiation. Two mice given foreign white blood cells are alive 120 days after irradiation, and three others have lived 60 days. All five show the presence of foreign (donor type) red and white blood cells in samples recently taken. It seems clear from this work that in the mouse, white blood cells can be used instead of bone marrow to prevent the acute radiation death caused by bone marrow failure. The amount of white blood cells required is considerably greater than when bone marrow is used. To use foreign white blood cells, special genetic relationships are needed.

Use was made of the bio-assay previously described to test spleen cells from semi-isologous chimeras for a secondary response by parental strain (P) mice against F_1 cells. This type of reaction was elicited only by spleen cells from 30-day-old chimeras in which the bone marrow graft was of P origin. This finding indicates that an immune reaction by donor against host cells was going on in this type of chimera. The fact that this reaction was concomitant with a mortality peak of the chimeras suggests the existence of an immunologic component in the pathogenesis of the secondary disease.

Mammalian Recovery: Mammalian Cytology and Genetics in Vitro. — Measurements of x-ray-induced chromosome-type aberration rates in leucocytes from freshly drawn human blood were completed. The aberration rates are the same as those observed in other systems. Measurements of x-ray-induced chromatid-type aberration rates in human leucocytes are being made. A launch-site test of the experiments for the BIOS-I (formerly NERV-II) space project was successfully completed.

Radiation Immunology. — The irradiated-animal in vivo culture technique has been employed to investigate the primary and secondary antibody response of a constant number of mouse spleen cells as a function of antigen dose. Decreasing the primary, preimmunizing antigen dose results in a reduced antibody response when a standard challenging (secondary) dose of antigen is given. The same is true when the time interval between preimmunization (constant antigen dose) and cell transfer is reduced. When a fixed number of equivalently preimmunized cells are transferred and the secondary, challenging antigen dose is varied, the antibody response is again delayed and/or reduced with decreasing amounts of antigen. These results indicate that antibody production is dependent upon the balance of two factors — cellular differentiation and maturation and cellular division. Experiments utilizing the above approach and combined with other techniques should reveal whether or not this is so.

Phagocytosis may be an initial cellular event in antibody production. The phagocytic activity of mouse peritoneal exudate cells with respect to erythrocytes of several species has been studied. When a mixture of two types of erythrocytes — one closely and one distantly related to the phagocytes — is studied, the more distantly related cells are preferentially engulfed. When the same mixture is studied in the presence of specific antiserum to the closely related erythrocyte, the latter is now preferentially phagocytized.

Initial experiments concerning the autoregulatory effect of preformed antibody on the synthesis of new antibody by spleen cells indicate that this feed-back mechanism is operative. Studies are in progress to further

analyze the extent to which this mechanism may govern antibody formation and the cellular differentiation which is believed to accompany antibody formation.

MOLECULAR- AND CELLULAR-LEVEL STUDIES

Cell Growth and Reproduction. — Amoebae have been stimulated to take up primer deoxyribonucleic acid (DNA) from the medium by induction of pinocytosis. The incorporation of H^3-thymidine into new DNA in the cytoplasm of such primer-fed cells has been demonstrated by autoradiography. The experiments are considered as evidence that the DNA polymerizing enzyme is not restricted to the cell nucleus but is distributed throughout the cytoplasm.

Biophysics: Ultraviolet Studies. — It has been shown that denatured DNA, in the presence of the four nucleoside triphosphates and an enzyme derived from calf thymus, acts as a primer for new DNA synthesis. The ability of ultraviolet-irradiated, denatured DNA to act as a primer was determined. The shapes of the dose-survival curves for 2800 and 2400 A irradiation are compatible with the idea that the dimers of thymine produced by ultraviolet light act as relative blocks to the polymerization of new DNA on the primer. The rate of polymerization past a block is ~1/100 of the normal rate. DNA formed from irradiated primer has a base composition different from that of DNA formed from unirradiated samples.

Biophysics: Vacuum Ultraviolet Studies. — Small numbers of spores of *Streptomyces griseus* have been dried on the surface of millipore filters. After irradiation, the filters are placed on nutrient agar, and the spores are permitted to form microcolonies. Inactivation on the filters by 250-kvp x rays is exponential, indicating the absence of clumping. Inactivation at 2537 A shows an extrapolation number of about 20 and the expected high photoreactivation. The beam from a 4-in., high-vacuum, magnetically constrained carbon arc (DCX), in argon at very low pressure, and filtered by lithium fluoride, produces exponential inactivation, with little or no photoreactivation. The radiation lies principally at 1548 A. Experiments are still preliminary, a serious complication at present being the rapid darkening of the LiF filters under irradiation.

Biophysics: Electron Spin Resonance Studies. — Very preliminary measurements of the possibility of correlating numbers of electron spin resonances produced by ionizing radiation with liberation of gas (probably hydrogen) have indicated that there are an order of magnitude more spins than gas molecules. A reflection cavity is being set up for low-temperature ESR studies and for ESR measurements during irradiation with visible and ultraviolet light.

RADIOLOGICAL PHYSICS, HEALTH PHYSICS, AND INSTRUMENTATION

Basic Instrumentation. — An infrared image converter, type 6032, can be used to detect infrared radiation to which silicon is transparent. The effective wavelengths are between 1.1 and 1.3 μ. By use of such a converter and a source of circularly polarized infrared light, the residual

stresses in several specimens of commercial float-zoned silicon were measured. Stresses as high as 1000 psi were observed.

Equipment for making controlled alloy junctions on silicon was installed. A new vacuum metal-evaporator system and an inert-atmosphere furnace permit the forming of shallow alloys on silicon for both "ohmic" contacts and p-n junctions.

A study was made of the optimum conditions for making p-i-n junction diodes by the lithium drift-compensation method. A system which incorporates the optimum conditions for rapid drift was set up.

An investigation to determine the properties of gold-doped silicon conductivity counters was begun. The use of gold-doped and of lithium-drifted silicon may make possible the construction of large-volume detectors.

OPEN LITERATURE PUBLICATIONS

Arnold, William, "Wave Mechanics and Muscular Contraction," J. Theoret. Biol. 1, 404 (1961).

Baldwin, W. H., and C. E. Higgins, "Complexes of Dibutyl Phosphoric Acid," J. Inorg. & Nuclear Chem. 17, 334 (1961).

Beaver, R. J., J. E. Cunningham, and R. C. Waugh, "Dispersions in Metals," p 142 in Uranium Dioxide: Properties and Nuclear Applications (ed. by J. Belle), Naval Reactors, Division of Reactor Development, U.S. Atomic Energy Commission, Washington, D.C., 1961.

Begun, G. M., and L. Landau, "Mass Spectra and Metastable Transitions in Isotopic Nitrous Oxides," J. Chem. Phys. 35, 547 (1961).

Berggren, R. G., "Neutron Irradiation Effects in Steels: Studies at Oak Ridge National Laboratory," p 370 in Steels for Reactor Pressure Circuits, Iron and Steel Institute Special Report No. 69 (1961).

Blewitt, T. H., R. R. Coltman, R. R. Jamison, and J. K. Redman, "Radiation Hardening in Copper Single Crystals," J. Nuclear Materials 2, 277 (1960).

Block, M. M., E. B. Brucker, R. Gessaroli, T. Kikuchi, A. Kovacs, C. M. Meltzer, R. Kraemer, M. Nussbaum, A. Pevsner, P. Schlein, R. Strand, H. O. Cohn, E. M. Harth, J. Leitner, L. Lendinara, L. Monari, and G. Puppi, "K^- Absorption in He^4. I. The Hyperon-Pion Resonance," Nuovo cimento 20, 724 (1961).

Cartledge, G. H., "The Comparative Roles of Oxygen and Inhibitors in the Passivation of Iron. IV. Osmium(VIII) Oxide," J. Phys. Chem. 65, 1361 (1961).

Cleland, J. W., and J. H. Crawford, Jr., "Radiation-Induced Disorder in Semiconductors," p 299 in Proceedings International Conference on Semiconductor Physics, Prague, 1960, Czechoslovak Academy of Sciences, Prague, 1961.

Coltman, R. R., T. H. Blewitt, and S. T. Sekula, "The Effects of Annealing in Oxygen on the Resistivity of High Purity Copper," p 72 in Colloque International sur les proprietes des metaux de tres haute purete (International Conference on High Purity Metals, Paris, France, Oct. 10-14, 1959), Centre National de la Recherche Scientifique, Paris, 1960.

Crawford, J. H., Jr., "Creation of Defects in Alkali Halide Crystals by Ionizing Radiation," p 21 in Proceedings of International Conference on Color Centers and Crystal Luminescence, Turin, Italy, Sept. 8-11, 1960 (ed. by G. Bonfiglioli) (1961).

Crouse, Helen V., "Irradiation of Condensed Meiotic Chromosomes in Lilium longiflorum," Chromosoma 12, 190 (1961).

Foard, D. E., and A. H. Haber, "Anatomic Studies of Gamma-Irradiated Wheat Growing Without Cell Division," Am. J. Botany 48, 438 (1961).

Gengozian, Nazareth, Rachel Carter, and W. J. Peterson, "Antibody Synthesis by Transplanted Heterologous Chimera Spleen Cells in Irradiated Recipients," J. Immunol. 87, 209 (1961).

Goodman, Joan W., and C. C. Congdon, "Blood-Marrow Mixtures in Irradiated Mice: Effect of Blood Injection on Bone Marrow Transplantation in Lethally Irradiated Mice," Arch. Pathol. 72, 18 (1961).

Grell, E. H., "Melanogaster – New Mutants," Drosophila Info. Serv. 34, 50 (1960).

Grimm, F. C., and D. G. Doherty, "Properties of the Two Forms of Malic Dehydrogenase from Beef Heart," J. Biol. Chem. 236, 1980 (1961).

Haber, A. H., W. L. Carrier, and D. E. Foard, "Metabolic Studies of Gamma-Irradiated Wheat Growing Without Cell Division," Am. J. Botany 48, 431 (1961).

Heusler, K. E., and G. H. Cartledge, "The Influence of Iodide Ions and Carbon Monoxide on the Anodic Dissolution of Active Iron," J. Electrochem. Soc. 108, 732 (1961).

Kopp, O. C., L. A. Harris, and G. W. Clark, "The Hydrothermal Conversion of Muscovite to Kalsilite and an Iron-Rich Mica," Am. Mineralogist 46, 719 (1961).

Kelley, G. G., N. H. Lazar, and O. B. Morgan, "A Source for the Production of Large DC Ion Currents," Nuclear Instr. and Methods 10, 263 (1961).

Mackin, R. J., Jr., "Plasma Accumulation in a Device Fed by Energetic Ion Trapping," Nuclear Fusion 1, 131 (1961).

Mans, R. J., and G. D. Novelli, "In Vitro Amino Acid Incorporation into Particle Protein from Maize Seedlings," Biochim. et Biophys. Acta 50, 287 (1961).

Mans, R. J., and G. D. Novelli, "Measurement of the Incorporation of Radioactive Amino Acids into Protein by a Filter-Paper Disk Method," Arch. Biochem. Biophys. 94, 48 (1961).

McDowell, W. J., and K. A. Allen, "Thorium Extraction by Di-n-decylamine Sulfate in Benzene," J. Phys. Chem. 65, 1358 (1961).

McHargue, C. J., "The Effect of Initial Orientation on the Fiber Texture of Aluminum Rods," Trans. Met. Soc. AIME 221, 812 (1961).

Nicoletti, Benedetto, "New Mutants – w^{cf}:White Coffee," Drosophila Info. Serv. 34, 52 (1960).

Nicoletti, Benedetto, and D. L. Lindsley, "Cytogenetic Analysis of T(X;Y)'s," Drosophila Info. Serv. 34, 95 (1960).

Odell, T. T., Jr., and A. C. Upton, "Late Effects of Internally Deposited Radioisotopes," pp 375–92 in Radioactive Isotopes in Physiology, Diagnostics, and Therapy (ed. by H. Schwiegk and F. Turba), 2d ed., Springer, Berlin, 1961.

Palko, A. A., J. S. Drury, and W. E. Bull, "Separation of Boron Isotopes. V. The Phenol-BF_3 System," J. Chem. Phys. 35, 103 (1961).

Parkinson, W. W., and D. Binder, "Post-Irradiation Oxidation and Molecular Weight Changes in Polystyrene and Polymethyl Methacrylate," p 224 in Materials in Nuclear Applications, ASTM-STP-276 (1960).

Phan The Tran and M. A Bender, "Preservation of Viable Bone Marrow by Freezing," pp 59–64 in Radiobiology, Proceedings of the Third Australasian Conference on Radiobiology Held at the University, Sydney, 15–18 August, 1960, by the Australian Radiation Society (ed. by P. L. T. Ilbery), Butterworths, London, 1961.

Prescott, D. M., "The Growth-Duplication Cycle of the Cell," pp 255–82 in International Review of Cytology, vol 11 (ed. by G. H. Bourne and J. F. Danielli), Academic Press, New York, 1961.

Rainey, R. H., and J. G. Moore, "Laboratory Development of the Acid Thorex Process for Recovery of Thorium Reactor Fuels," Nuclear Sci. and Eng. 10, 367 (1961).

Sandler, L., P. Hart, and Benedetto Nicoletti, "Phenotypic Changes Associated with Chromosome Rearrangements at the y Locus," Drosophila Info. Serv. 34, 103 (1960).

Smith, P. E., R. Bibaud, G. S. Sadowski, J. C. Bresee, D. L. Foster, J. T. Long, J. Ullmann, A. R. Irvine, W. E. Unger, J. McClendon, J. Wachter, J. K. Davidson, A. C. Schafer, Jr., R. B. Lemon, C. E. Stevenson, J. A. Buckham, J. Dunn, H. M. Jones, and R. Geier, "Equipment Design – Process and Mechanical Considerations," p 536 in Reactor Handbook, vol II (ed. by S. M. Stoller and R. B. Richards), Interscience, New York, 1961.

Thoma, R. E., and T. S. Carlton, "Phase Equilibria in the System $CsF-ThF_4$," J. Inorg. & Nuclear Chem. 17, 88 (1961).

Thoma, R. E., C. F. Weaver, H. A. Friedman, H. Insley, L. A. Harris, and H. L. Yakel, Jr., "Phase Equilibria in the System $LiF-YF_3$," J. Phys. Chem. 65, 1096 (1961).

Upton, A. C., "The Dose-Response Relation in Radiation-Induced Cancer," Cancer Research 21, 717 (1961).

von Borstel, R. C., "Postmeiotic Nuclear Behavior in Uninseminated Eggs of Drosophila melanogaster," Drosophila Info. Serv. 34, 110 (1960).

Waugh, R. C., J. E. Cunningham, and R. J. Beaver, "Aluminum-Uranium Oxide Reaction," p 364 in Uranium Dioxide: Properties and Nuclear Applications (ed. by J. Belle), Naval Reactors, Division of Reactor Development, U.S. Atomic Energy Commission, Washington, D.C., 1961.

Welshons, W. J., "New Mutants:In(1)pdf:pod-foot," Drosophila Info. Serv. 34, 54 (1960).

Whiting, Anna R., "Temperature Effects on Lethal Mutation Rates of Habrobracon Oocytes X Irradiated in First Meiotic Metaphase," Genetics 46, 811 (1961).

Wolff, Sheldon, "Some Aspects of Radiation Genetics," pp 419–75 in Mechanisms in Radiobiology, vol I (ed. by M. Errera and A. Forssberg), Academic Press, New York, 1961.

Zeldes, Henry, and Ralph Livingston, "A Paramagnetic Species in Irradiated $NaNO_2$," J. Chem. Phys. 35, 563 (1961).

VISITORS

UNITED STATES

Advisory Committee for the Metallurgy Division

Burr, A. A.
Johnson, J. R.
Smith, C. S.
Smoluchowski, R.

FOREIGN

Name	Affiliation	Citizen of
Alder, K.	Australian AEC	Australia
Anderson, A. J.	Danish AEC	Denmark
Appel, H. F.	T. H. Karlsruhe	Germany
Asada, K.	Kyoto University	Japan
Bacon, G. E.	Atomic Energy Research Establishment, Harwell	Great Britain
Barbier, M.	CERN, Switzerland	France
Bernot, N. Z.	Nuclear Institute Jozef Stefan	Yugoslavia
Bhalla, C. P.	Westinghouse Electric Co.	India
Bleaney, B.	Clarendon Laboratory	Great Britain
Blennemann, D.	University of Bonn	Germany
Caglioti, V.	University of Rome	Italy
Charlton, J. C.	Radiochemical Centre	Great Britain
Fariwar-Sadri, N.	Tehran University	Iran
Fer, F.	ORSAY, Paris	France
Fradin, J.	French CEA	France
Fritze, K.	McMaster University	Germany
Gabrovsek, Z.	Nuclear Institute Jozef Stefan	Yugoslavia
Gelin, P.	French CEA	France
Genuardi, G.	EURATOM, Brussels	Italy
Glavic, V.	Nuclear Institute Jozef Stefan	Yugoslavia
Hagedoorn, H. L.	Philips Research Laboratory	Holland
Healy, T. V.	United Kingdom AEA	United Kingdom
Herdade, S. B.	Instituto de Energia Atomica	Brazil
Hewitt, A. G.	Rutherford Laboratory	Great Britain
Hobbis, L. C. W.	Rutherford Laboratory	New Zealand
Hyodo, T.	Kyoto University	Japan
Jensen, B. S.	Danish AEC	Denmark
Johnson, A. A.	Imperial College	Great Britain
Johnson, A. E.	National Engineering Laboratory, Scotland	United Kindgom
Jones, E. J.	Rutherford Laboratory	Great Britain
Kamijo, F.	Showa Electrochemical Co. Ltd.	Japan
Katz, L.	University of Saskatchewan	Canada
Kennett, T. J.	McMaster University	Canada

Name	Affiliation	Citizen of
Kishida, J.	Asahi Science Monthly	Japan
Kobayashi, K.	University of Tokyo	Japan
Lapostolle, P.	CERN, Switzerland	France
Lauer, K. F.	EURATOM	Germany
Mahfouz, M.	United Arab Republic AEE	United Arab Republic
Meunier, R.	French CEA	France
Mishimura, I.	Asahi Science Monthly	Japan
Nam, N. H.	Atomic Energy Office of Viet Nam	Viet Nam
Newman, R. C.	Associated Electrical Industries	United Kingdom
Nishiwaki, N.	University of Tokyo	Japan
Otte, H. M.	RIAS, Division of The Martin Co.	Great Britain
Oudar, J.	University of Paris	France
Pelce, J.	French CEA	France
Pisanski, C.	Nuclear Institute Jozef Stefan	Yugoslavia
Quijandria, B.	SIPA-Department of Agricultural Research	Peru
Saiki, M.	University of Tokyo	Japan
Schmeissner, F.	CERN	Germany
Schmidt, E.	Chamber of Commerce, Basle, Switzerland	Switzerland
Sennis, C.	CNEN	Italy
Sens, P. F.	Reactor Centrum Nederland	Holland
Trembley, J.	CERN	Switzerland
Uffelmann, F. L.	British Embassy	United Kingdom
Vogt-Nilsen, N.	CERN, Switzerland	Norway
Zarzycki, J.	Saint Goban, Paris	

Reports issued in this series during the past year:

September 1960	ORNL-3024
October 1960	ORNL-3038
November 1960	ORNL-3048
December 1960	ORNL-3062
January 1961	ORNL-3074
February 1961	ORNL-3097
March 1961	ORNL-3120
April 1961	ORNL-3140
May 1961	ORNL-3149
June 1961	ORNL-3156
July 1961	ORNL-3174
August 1961	ORNL-3190

ORNL-3211
C-44a – Nuclear Technology – Materials
M-3679 (25th ed.)

INTERNAL DISTRIBUTION

1. I. Alexeff
2. C. F. Baes
3. E. A. Bagley
4. P. S. Baker
5. C. R. Baldock
6. L. H. Barker
7. S. E. Beall
8. E. E. Beauchamp
9. R. H. Beidel
10. P. R. Bell
11. D. S. Billington
12. C. A. Blake
13. R. E. Blanco
14. F. F. Blankenship
15. E. P. Blizard
16. J. O. Blomeke
17. A. L. Boch
18. E. G. Bohlmann
19. C. J. Borkowski
20. G. E. Boyd
21. M. A. Bredig
22. J. C. Bresee
23. R. B. Briggs
24. R. E. Brooksbank
25. K. B. Brown
26. F. R. Bruce
27. W. D. Burch
28. T. H. J. Burnett
29. A. D. Callihan
30. A. E. Cameron
31. C. E. Center (K-25)
32. T. E. Cole
33. C. F. Coleman
34. E. L. Compere
35. D. D. Cowen
36. J. A. Cox
37. F. L. Culler
38. J. E. Cunningham
39. J. S. Drury
40. A. C. England
41. M. F. Fair
42. D. E. Ferguson
43. J. L. Fowler
44. J. H. Frye, Jr.
45. J. L. Gabbard (K-25)
46. W. F. Gauster
47. M. W. Gerrard
48. J. H. Gillette
49. W. Y. Gissel
50. H. E. Goeller
51. C. D. Goodman
52. A. T. Gresky
53. J. C. Griess
54. W. R. Grimes
55. P. A. Haas
56. C. S. Harrill
57. J. C. Hart
58. M. R. Hill
59. C. J. Hochanadel
60. A. Hollaender
61. L. B. Holland
62. R. W. Horton
63. F. T. Howard
64. A. S. Householder
65. H. H. Hubbell
66. G. S. Hurst
67. G. H. Jenks
68. R. W. Johnson
69. R. J. Jones
70. W. H. Jordan
71. P. R. Kasten
72. G. W. Keilholtz
73. G. G. Kelley
74. M. T. Kelley
75. E. M. King
76. W. C. Koehler
77. K. A. Kraus
78. Laboratory Shift Supervisor (D. Phillips)
79. J. A. Lane
80. D. M. Lang (K-25)
81. C. E. Larson
82. R. E. Leuze
83. W. H. Lewis
84. T. A. Lincoln
85. S. C. Lind
86. R. B. Lindauer
87. R. S. Livingston
88. J. T. Long
89. L. O. Love

90. R. N. Lyon
91. R. J. Mackin
92. H. G. MacPherson
93. F. C. Maienschein
94. W. D. Manly
95. J. A. Martin
96. H. F. McDuffie
97. J. R. McNally
98. A. J. Miller
99. E. C. Miller
100. K. Z. Morgan
101. W. L. Morgan
102. F. J. Muckenthaler
103. E. J. Murphy
104. J. P. Murray (K-25)
105. M. L. Nelson
106. C. E. Normand
107. G. W. Parker
108. R. B. Parker
109. J. J. Pinajian
110. M. E. Ramsey
111. A. W. Riikola
112. L. P. Riordan
113. A. F. Rupp
114. A. D. Ryon
115. H. C. Savage
116. H. W. Savage
117. A. W. Savolainen
118. H. E. Seagren
119. E. D. Shipley
120. A. Simon
121. O. Sisman
122. J. R. Sites
123. M. J. Skinner
124. A. H. Snell
125. W. S. Snyder
126. W. L. Stirling
127. R. W. Stoughton
128. H. Stringfield
129. E. G. Struxness
130. J. C. Suddath
131. W. H Sullivan
132. C. D. Susano
133. J. A. Swartout
134. E. H. Taylor
135. C. D. Watson
136. B. S. Weaver
137. A. M. Weinberg
138. M. E. Whatley
139. J. C. White
140. C. E. Winters
141. E. O. Wollan
142. R. E. Worsham
143. W. Zobel
144. A. Zucker
145-146. Central Research Library
147. ORNL — Y-12 Technical Library, Document Reference Section
148. Reactor Division Library
149. Biology Library
150-337. Laboratory Records Department
338. Laboratory Records, ORNL R.C.

EXTERNAL DISTRIBUTION

339-375. Division of Research and Development, AEC, ORO
376. Aeroprojects, Inc. (W. B. Tarpley)
377. Allis-Chalmers Manufacturing Co. (W. F. Banks)
378-380. Ames Laboratory: Iowa State College (F. H. Spedding)
381-383. Argonne National Laboratory (N. S. Hilberry)
384. Atomics International (H. Pearlman)
385. Babcock and Wilcox Co. (Atomic Energy Division)
386-387. Battelle Memorial Institute (H. W. Russell)
388-390. Brookhaven National Laboratory (M. Goldhaber)
391. Bureau of Mines, Salt Lake City (J. B. Clemmer)
392-393. Division of Research and Development, AEC, ORO (D. F. Cope)
394-401. General Atomic (General Dynamics Corp.) (Manager)
402-403. General Nuclear Engineering Corp. (J. West)
404-405. Idaho Chemical Processing Plant (R. L. Doan)
406. Kaiser Engineers (P. D. Bush)
407-408. Knolls Atomic Power Laboratory (K. R. Van Tassell)
409-410. Lawrence Radiation Laboratory (H. Fidler)

411-412. Los Alamos Scientific Laboratory (N. E. Bradbury)
413-414. National Bureau of Standards (L. S. Taylor)
415. National Lead Company (C. K. McArthur)
416. Nuclear Metals, Inc. (A. R. Kaufmann)
417-418. Philadelphia Electric Co. (L. R. Gaty)
419. Sanderson and Porter (Atomic Energy Division)
420. Union Carbide Corporation (R. W. McNamee)
421-422. USAEC, Chicago Operations Office
423. USAEC, Lockland Aircraft Reactors Operations Office (H. H. Gorman)
424-425. USAEC, San Francisco Operations Office (R. Hughey)
426-427. USAEC, Savannah River Operations Office (H. Rahner)
428. Westinghouse Electric Corp. (A. Squire)
429-676. Given distribution as shown in M-3679 (25th ed.) category C-44a and those addresses shown in C-44b and C-44c which do not receive copies under C-44a